Optimal Design and Effective Control of Triple-Column Extractive Distillation for Separating Ethyl Acetate/Ethanol/Water with Multi-Azeotrope

Ao Yang[1], Hechen Zou[1], I-Lung Chien[2], Dan Wang[1], Shun'an Wei[1], Jingzheng Ren[3] and Weifeng Shen[1,*]

[1]School of Chemistry and Chemical Engineering, Chongqing University, Chongqing 400044, P. R. China

[2]Department of Chemical Engineering, National Taiwan University, Taipei 10617, Taiwan

[3]Department of Industrial and Systems Engineering, The Hong Kong Polytechnic University, Hong Kong SAR, China

Corresponding Author: *(W.S) E-mail: shenweifeng@cqu.edu.cn

Abstract: The separation of ternary non-ideal system ethyl acetate (EtAC)/ethanol (EtOH)/water with multiazeotropes is very important since they are always generated in the production process of *n*-butanol synthesis from ethanol, which is much more difficult due to the formation of multi-azeotrope and distillation boundary. Herein, a systematic conceptual design, optimization and control approach for ternary extractive distillation of multi-azeotrope mixtures EtAC/EtOH/water is proposed. In the procedure involves entrainer screening, conceptual design, global optimization, process evaluation and robust control strategy. The optimization results demonstrate that the total annual cost, exergy loss and carbon dioxide emissions of the proposed triple-column extractive distillation are significantly reduced compared with those of the existing process. Dynamic performances illustrate that the improved dual temperature and feedforward control strategy can well handle the three product purities while two kinds of disturbances (*i.e.*, feed flow rate and composition) are introduced.

Keywords: ternary extractive distillation; optimization; multi-azeotrope; dynamic control; separation

1. Introduction

It is generally known that ethyl acetate (EtAC) and ethanol (EtOH) are frequently used as organic solvent and raw material in the biochemical and pharmaceutical industries.[1, 2] EtAC/EtOH mixtures are generated with water in the process of *n*-butanol synthesis (*i.e.*, ethanol-to-butanol).[3] However, the ternary mixture EtAC/EtOH/water is a complex system with three binary azeotropes (*i.e.*, EtAC/EtOH, EtOH/water and EtAC/water azeotropes) and a ternary azeotrope (*i.e.*, EtAC/EtOH/water) at atmospheric pressure, which lead to the separation of such non-ideal azeotropic system more difficult than that of other mixtures with one azeotrope *via* conventional distillations.[3-5] Therefore, developing an energy-saving process is necessary for the recovery of valuable solvents from waste liquid from the perspective of sustainable development.[6]

Several unconventional distillation schemes such as azeotropic distillation[7-11], pressure-swing distillation[12-16] and extractive distillation[17-23] are extensively applied for separating azeotropic or close-boiling system. Extractive distillation is frequently applied for azeotropic or close-boiling mixtures of separation by adding a third component (denoted as entrainer) to break the azeotrope and increase the relativity volatility of these mixtures. For example, an energy-efficient extractive distillation scheme by changing operating pressure for separating azeotropic system acetone/methanol using entrainer dimethyl sulfoxide (DMSO) is investigated by You et al.[18]. Shen et al.[19] reported a novel design method of an extractive distillation separation sequence for maximum-boiling azeotropes by using heavy entrainers. Lo and Chien[20] studied an efficient scheme for separating of *tert*-butanol/water azeotropic mixtures *via* the extractive distillation. An energy-saving extractive distillation scheme with or without heat integration for separating tetrahydrofuran/water azeotropic system is explored by Gu et al.[24]. Moreover, dividing wall column technology is extended to the extractive distillation achieving energy efficiency by Kiss and Ignat.[25].

Extractive dividing wall column is then reported by Sun et al.[26] for benzene/cyclohexane separation. Recently, extractive distillations are extended to separate ternary mixtures with one (or more) azeotrope(s). For instance, Timoshenko et al.[27] explored several extractive distillation processes for the separation of ternary systems with one or multi-azeotrope(s) and then they evaluated the applicability of the extractive distillation sequences with the thermally coupled configurations. Yang et al.[28] reported a decanter assisted extractive dividing wall column configuration to separate ternary azeotropic system methanol/toluene/water with multi-azeotrope, which can save up to 15.14% saving of total annual cost (TAC). Three alternative ternary extractive distillation sequences for the separation of multi-azeotrope system tetrahydrofuran/ethanol/water are explored by Zhao et al.[29]. Subsequently, this mixture is separated *via* the thermally coupled configuration.[21] For the separation of benzene/cyclohexane/toluene system, the thermally coupled ternary extractive distillation is explored by Luyben.[30]. Different thermally coupled separation configurations (*e.g.*, side-stream) are reported for separating ternary system acetonitrile/benzene/methanol with multi-azeotrope.[22]

Entrainer screening is extremely important to design an efficient extractive distillation process.[31, 32] A suitable entrainer could effectively reduce energy consumption in the extractive distillation.[31] Some criteria are proposed to get a feasible candidate entrainer for the azeotrope system. Recently, Zhang et al.[2] explored an appropriate method for the separation of EtAC and EtOH azeotropic system and then they showed the entrainer DMSO is better than ethylene glycol (EG). Hsu et al.[31] reported a very simple procedure for a quick comparison of alternative entrainer candidates before conducting rigorous process simulation. Petlyuk et al.[5] proposed an approach for the search and identification of possible splits of extractive distillations in ternary azeotropic system and the method of infinitely sharp splits using propylene glycol (PG) as entrainer for the separation of ternary mixtures EtAC/EtOH/water.

Recently, the separation of ternary azeotropic system EtAC/EtOH/water through four-column extractive distillation (FCED) process is proposed by Michaels et al.[3], inspired from which, we propose a systematic approach to design, optimize and control for the separation of ternary mixtures EtAC/EtOH/water by using the triple-column extractive distillation (TCED). In this study, we first propose an energy-saving TCED sequence to separate ternary azeotropic system EtAC/EtOH/water. Next, a short-cut method is proposed to screen the best entrainer from the candidates through the comparison of distance of iso- and uni- volatility lines and target component. The TCED sequence is optimized *via* the complete process optimization model. Finally, a robust control scheme with dual temperature and feedforward strategy is designed to well handle the product purities when the feed flowrate and composition disturbances are introduced.

2. Existing process for separating multi-azeotrope system EtAC/EtOH/water

To achieve the separation of ternary system EtAC/EtOH/water with four azeotropes[33], the FCED scheme (see Figure 1) using two entrainers (DMSO and EG) has been proposed by Michaels et al.[3]. The product EtAC is obtained by introducing an entrainer DMSO to break the two azeotropes between EtAC/water and EtAC/EtOH in the first extractive distillation column (*i.e.*, EDC1) while the entrainer is then recovered in the bottom of ERC1. Next, the top stream (D_2) of the first entrainer recovery column (ERC1) and the entrainer EG are respectively fed to the lower and upper stages of the extractive section of the second extractive distillation column (EDC2) to obtain the overhead product EtOH. Finally, the mixtures of water and EG are separated in the second entrainer recovery column (ERC2).

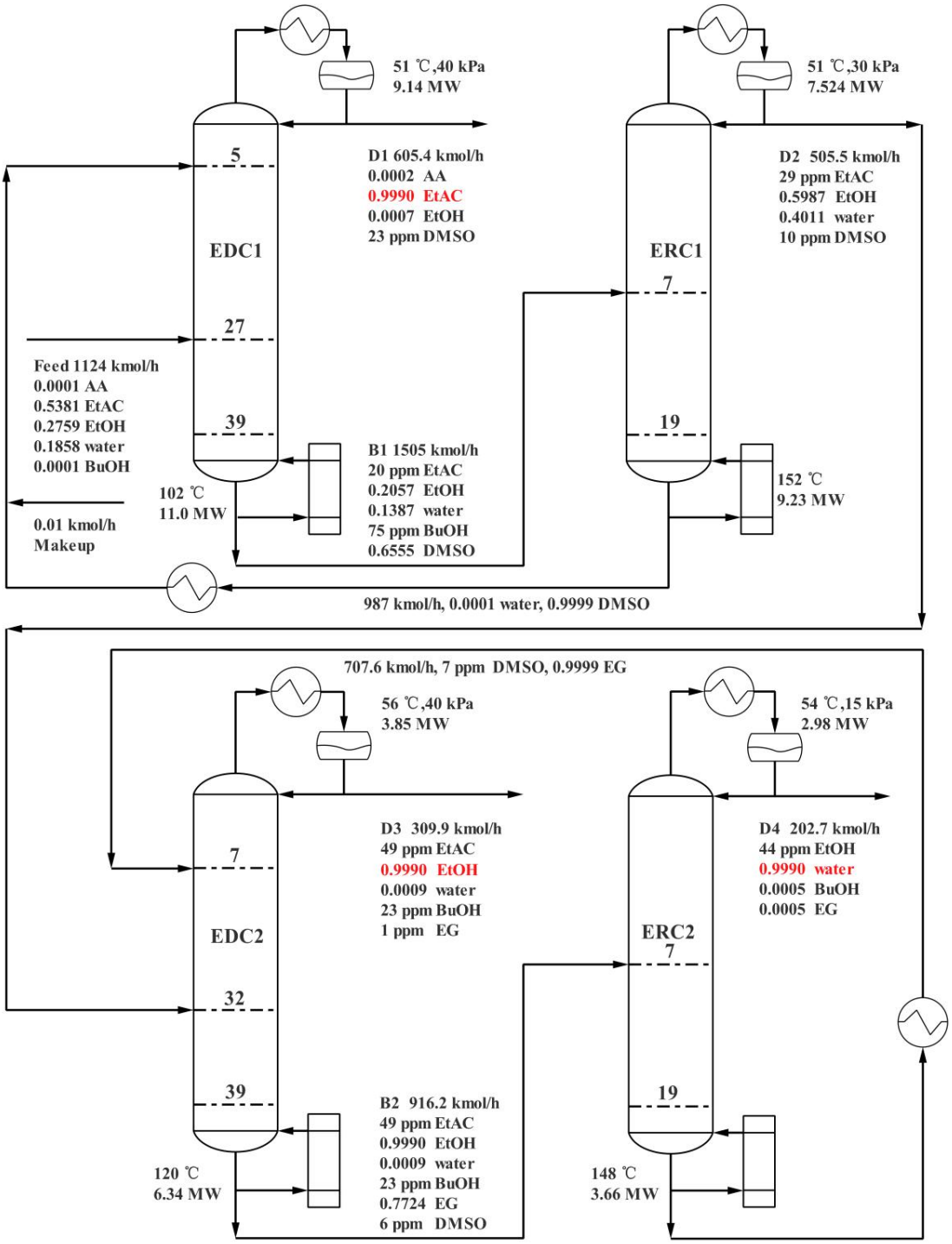

Figure 1. Existing FCED process for separating ternary mixtures EtAC/EtOH/water with multi-azeotrope

3. Methodology

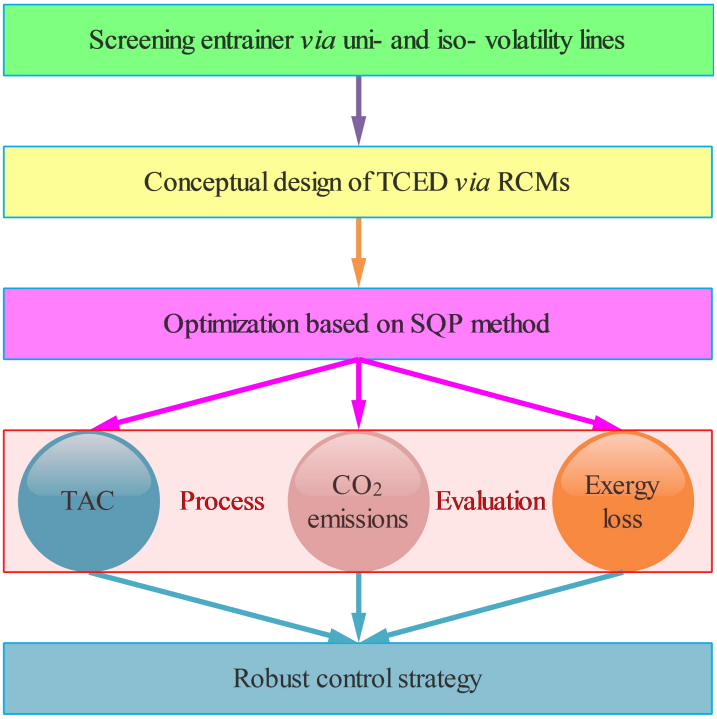

Figure 2. Proposed procedure for the design, optimization and dynamic control of EtAC/EtOH/water separation using TCED process

A systematic procedure for design and control of the ternary azeotropic system EtAC/EtOH/water separation *via* the TCED process is shown in Figure 2. The proposed systematic approach is conducted in five steps. Step 1: a best suitable entrainer for the separation is screened by iso- and uni- volatility lines; Step 2: the thermodynamic feasibility insight and conceptual design for separating ternary azeotropic system is analyzed *via* residue curve maps (RCMs) and iso-volatility line; Step 3: the proposed process is optimized based on the sequential quadratic solver (SQP) solver; Step 4: three indicators TAC, CO_2 emissions and exergy loss are introduced to evaluate and compare the proposed and existing processes; Step 5: A robust dual temperature and feedforward control strategy for the TCED process is proposed to well handle the products purities.

3.1 Entrainer screening

In this study, the separation of azeotrope mixtures (*i.e.*, EtOH/EtAC, EtOH/water and EtAC/water) with a heavy entrainer (E) belongs to the class 1.0-1a of Serafimov's classification.[34-36] The general feasibility criterion for the separation of non-ideal systems incorporating with the RCMs and iso-volatility line is illustrated in Figure 3.

The proportion of vapor and liquid equilibrium concentration for component *i* (*i.e.*, y_i and x_i) is denoted as distribution coefficient (K_i), which is defined in Eq. 1.

$$K_i = \frac{y_i}{x_i} \tag{1}$$

Eq. 2 gives the relative volatility α_{ij}, which is the ratio distribution coefficient of components *i* and *j*.

$$\alpha_{ij} = \frac{y_i / x_i}{y_j / x_j} \tag{2}$$

The relative volatility features the ability of component *i* to transfer (evaporate) into the vapor phase compared to the ability of component *j*. Component *i* is more volatile than component *j* if $\alpha_{ij} > 1$ and less volatile if $\alpha_{ij} < 1$. In this study, the iso-volatility curves ($\alpha_{ij} = 1$) are obtained *via* the *Distillation Synthesis* tools of Aspen Plus. Uni-volatility curves ($\alpha_{ij} \neq 1$) could be obtained *via* the Flash2 module.[31]

For the extractive distillation scheme, a suitable entrainer indicates low energy consumption. The iso-volatility curve $\alpha_{AB} = 1$ intersects the binary side B-E or C-E while the intersection point is also called x_P which can be used to evaluate the efficiency of entrainer.[31] The closer the intersection to target component (i.e., small value of x_P), the less amount of entrainer is required indicating lower energy and capital costs.[18]

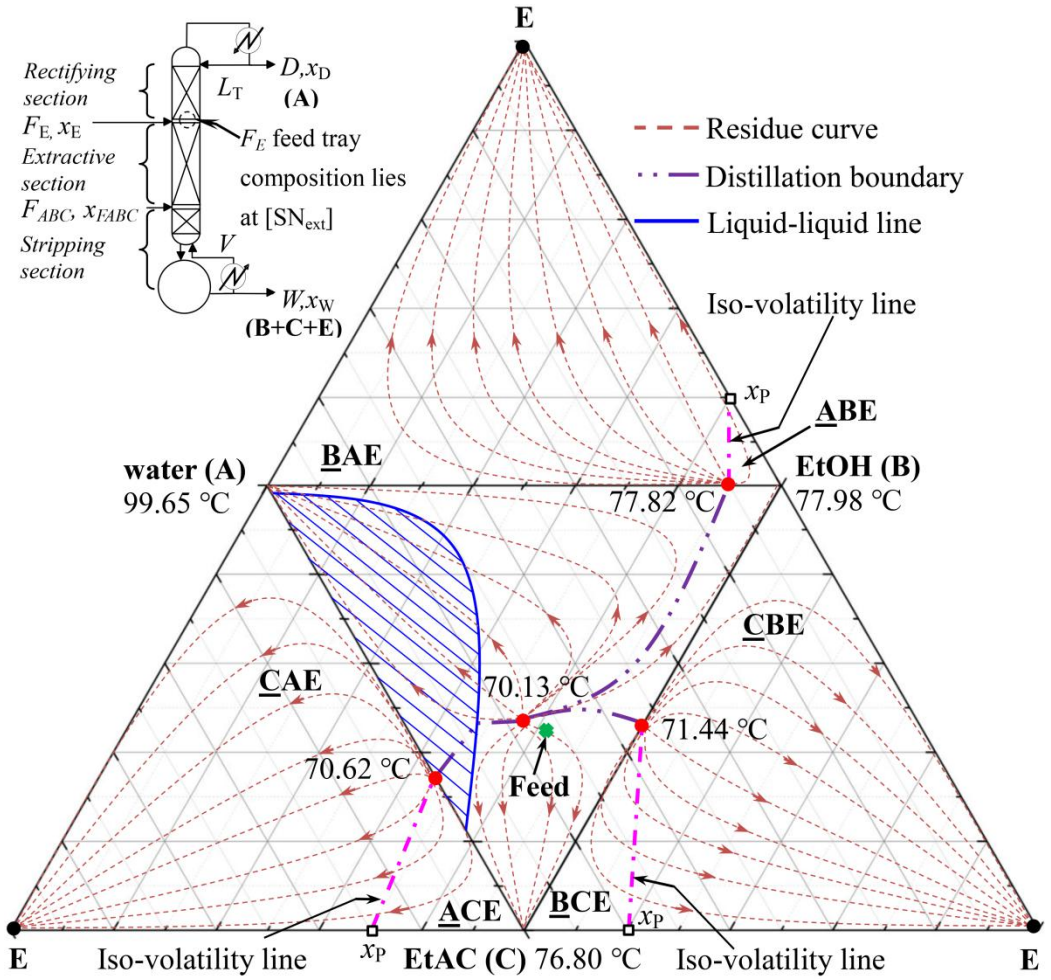

Figure 3. Extractive distillation configuration and thermodynamic features of class 1.0-1a at 100 kPa

3.2 Conceptual design

The iso-volatility curve $\alpha_{AB} = 1$ curve divides the ternary diagram (ABE) into two regions, the volatility orders are **B**AE in the left region and **A**BE in the right region (see Figure 3). In this work, the volatility order **B**AE indicates that B is the first possible distillate product in this section. The feasibility region **A**BE of this class is located in the lower part of the ternary diagram.[37-39] Similar analysis can be carried out for the volatility order **C**AE and **C**BE. Only when the entrainer flow rate is larger than this minimum value, the separation is feasible and the component A could be obtained at the distillate stream by a direct column configuration. As a result, the minimum entrainer flow rate is the vital lower boundary when optimizing the extractive distillation process.

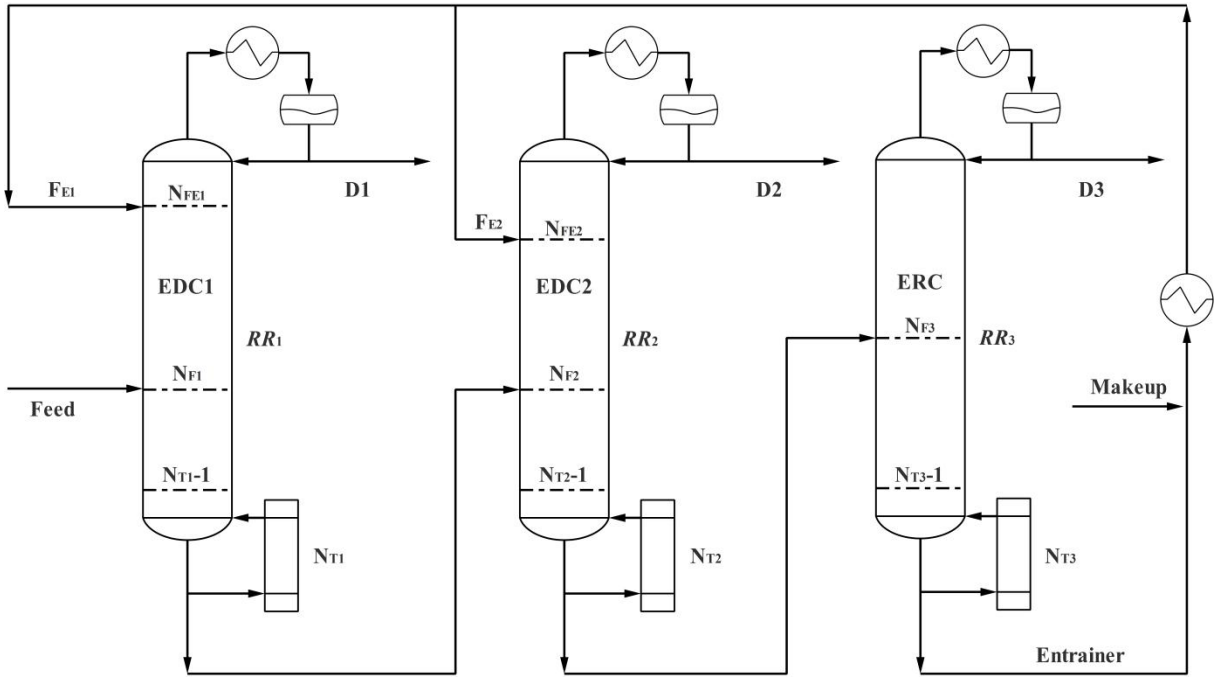

Figure 4. Conceptual design process for separating EtAC/EtOH/water mixture using TCED

The conceptual design process for separating EtAC/EtOH/water mixture using TCED is illustrated in Figure 4. Three products are obtained as distillate in three columns EDC1, EDC2, and ERC, respectively. The optimal feed locations (*i.e.*, N_{FE1}, N_{FE2}, N_{F1}, N_{F2} and N_{F3}), reflux ratios (*i.e.*, RR_1, RR_2 and RR_3), and entrainer flowrate (F_{E1} and F_{E2}) are obtained by the below optimization section.

3.3 Process optimization

Herein, the complete process optimization model (**CPOM**) based on SQP solver[40, 41] is proposed to optimize the proposed process, it is implemented in the Aspen Plus by following two steps,

Step 1: the convergence of the optimization process could be easy achieved for the flowsheet of open-loop, the proposed **CPOM** is employed with TAC as an objective function by manipulating 16 variables under specified purities to obtain optimal operating conditions.

Step 2: the optimized operating conditions are then validated by running the Aspen Plus

simulator in the closed-loop flowsheet where the entrainer is recycled from the bottom stream of the entrainer recovery column (ERC) to the upper extraction section of the EDC1 and a makeup entrainer is added.

3.3.1 Objective function

In this work, TAC is introduced to optimize the proposed TCED process. According to our previous work[14, 28], TAC is sensitive to the key operational variables (see Eq. 3).

$$\begin{aligned}\min\ \mathrm{TAC} = f(&N_{\mathrm{T1}}, N_{\mathrm{T2}}, N_{\mathrm{T3}}, N_{\mathrm{F1}}, N_{\mathrm{F2}}, N_{\mathrm{F3}}, N_{\mathrm{FE1}}, N_{\mathrm{FE2}}, RR_1, RR_2,\\ &RR_3, D_1, D_2, D_3, F_{\mathrm{E1}}, F_{\mathrm{E2}})\end{aligned} \tag{3}$$

where N_{T1}, N_{T2}, and N_{T3} are respectively total stages of the columns EDC1, EDC2 and ERC; N_{F1}, N_{F2}, N_{F3}, N_{FE1} and N_{FE2} represent feed locations of fresh feed and entrainer, respectively; RR_1, RR_2 and RR_3 denote the reflux ratios of three columns; D_1, D_2 and D_3 stand for the distillate rates of three columns; F_{E1} and F_{E2} are the entrainer flow rates of two columns.

3.3.2 Constraints

Desired product purities are respectively defined in Eqs. 4–7, which are executed as constraint function in Aspen Plus.

$$x_{\mathrm{EtAC}} \geq x_{\mathrm{EtAC}}^{\mathrm{specified}} \tag{4}$$

$$x_{\mathrm{EtOH}} \geq x_{\mathrm{EtOH}}^{\mathrm{specified}} \tag{5}$$

$$x_{\mathrm{water}} \geq x_{\mathrm{water}}^{\mathrm{specified}} \tag{6}$$

$$x_{\mathrm{Entrainer}} \geq x_{\mathrm{Entrainer}}^{\mathrm{specified}} \tag{7}$$

where three threshold product purities are 99.90 mol% and the threshold recovery entrainer purity is 99.99 mol%.

In addition, some other rigorous constraints including mass balance, energy balance and thermodynamic relations are implicitly in Aspen Plus, which are demonstrated in Eqs. 8–9.[19]

$$h(x) = 0 \tag{8}$$

$$g(x) \leq 0 \tag{9}$$

3.3.3 Variable bounds

Lower and upper bounds of eight discrete variables (see Eqs. 10–17) and continuous variables (see Eqs. 18–25) are respectively obtained through the sensitivity analysis, which is inspired by Santaella et al.[42]. To achieve the global optimization, discrete and continuous variables are defined in the *Sensitivity/Vary* and *Optimization/Vary* of *Sensitively Analysis Tools*, respectively.

Discrete variables:

$$N_{T1}^{min} \leq N_{T1} \leq N_{T1}^{max} \tag{10a,b}$$

$$N_{T2}^{min} \leq N_{T2} \leq N_{T2}^{max} \tag{11a,b}$$

$$N_{T3}^{min} \leq N_{T3} \leq N_{T3}^{max} \tag{12a,b}$$

$$N_{F1}^{min} \leq N_{F1} \leq N_{F1}^{max} \tag{13a,b}$$

$$N_{FE1}^{min} \leq N_{FE1} \leq N_{FE1}^{max} \tag{14a,b}$$

$$N_{F2}^{min} \leq N_{F2} \leq N_{F2}^{max} \tag{15a,b}$$

$$N_{FE2}^{min} \leq N_{FE2} \leq N_{FE2}^{max} \tag{16a,b}$$

$$N_{F3}^{min} \leq N_{F3} \leq N_{F3}^{max} \tag{17a,b}$$

Continuous variables:

$$RR_1^{min} \leq RR_1 \leq RR_1^{max} \tag{18a,b}$$

$$RR_2^{min} \leq RR_2 \leq RR_2^{max} \tag{19a,b}$$

$$RR_3^{min} \leq RR_3 \leq RR_3^{max} \tag{20a,b}$$

$$F_{E1}^{min} \leq F_{E1} \leq F_{E1}^{max} \tag{21a,b}$$

$$F_{E2}^{min} \leq F_{E2} \leq F_{E2}^{max} \tag{22a,b}$$

$$D_1^{min} \leq D_1 \leq D_1^{max} \tag{23a,b}$$

$$D_2^{min} \leq D_2 \leq D_2^{max} \tag{24a,b}$$

$$D_3^{min} \leq D_3 \leq D_3^{max} \tag{25a,b}$$

Herein, the optimization model involving objective function (*i.e.*, TAC), constraints (*e.g.*, x_{D1} and x_{D2}) and variable bounds (*e.g.*, N_{T1} and RR_1) is defined as complete process optimization model

(**CPOM**) for the optimization of the proposed TCED process (see in Eqs. 3–25).

3.4 Economic, exergy loss, and CO_2 emissions evaluations

TAC involves two parts: operating and capital costs, which is proposed by Douglas[43] and given in Eq. 26.

$$\mathrm{TAC} = \frac{\mathrm{TCC}}{\mathrm{PP}} + \mathrm{TOC} \tag{26}$$

where the TCC denotes the total capital cost of the main equipment (*e.g.*, reboiler, condenser and column trays); the TOC illustrates total operating cost of the utilities (*i.e.*, cooling water and steam). Following the suggestion of Turton[44], the shorter the payback period (PP), the more profitable the project. Therefore, PP of three years is taken for calculating the capital investment in TAC.[44, 45] In addition, the calculation of cost in vacuum system is reported by Seider et al.[46]. The detailed calculation of economic parameters and equipment sizing are summarized in Table S1.

The energy efficiency is another significant indicator to evaluate the proposed process.[13] For a given system, the exergy loss (El) is defined as Eq. 27, which shows the difference value between total input and output of exergy.

$$\mathrm{El} = \sum \mathrm{E}x_{\mathrm{input}} - \sum \mathrm{E}x_{\mathrm{output}} \tag{27}$$

E*x* is illustrated as exergy in Eq. 28, for a given specified system which is computed *via* the enthalpy (H) and entropy (S).

$$\mathrm{E}x = (\mathrm{H} - \mathrm{H}_0) - \mathrm{T}_0 \cdot (\mathrm{S} - \mathrm{S}_0) \tag{28}$$

where the $(H-H_0)$ and $(S-S_0)$ represent the enthalpy and entropy difference between the specified and the reference systems and the environment temperature (i.e., 25 °C) is denoted as T_0.

To explore the environmental impact and sustainability of the proposed process, CO_2 emissions are introduced.[47-50] The evaluation of CO_2 emissions in distillation processes is a complex

issue because of the energy required (*i.e.*, steam) for reboiler could be produced from the conventional energy resources (*e.g.*, heavy fuel oil, coal and natural gas). Smith and Delaby[48] reported energy targets to compute the gas emissions (*e.g.*, CO_2) from the steam system by considering the typical process industry utility devices such as boiler and furnaces. Following that, a simple computation model of CO_2 emissions (see Eq. 29) for distillation scheme is presented by Gadalla et al.[49].

$$(CO_2)_{\text{emissions}} = (\frac{Q_{\text{fuel}}}{\text{NHV}}) \times (\frac{\text{C\%}}{100})\alpha \tag{29}$$

where α of 3.67 is the ratio of molecular weight between CO_2 and C, NHV denotes the net heating value (NHV = 39771 kJ/kg) and C% represents the carbon content and its value is 86.5 kg/kg.[49] The energy consumption of fuel (Q_{fuel}, kJ) is calculated as follows,

$$Q_{\text{fuel}} = \frac{Q_{\text{seq}}}{\lambda_{\text{seq}}} \times (h_{\text{seq}} - 419) \times (\frac{T_{\text{F}} - T_0}{T_{\text{F}} - T_{\text{S}}}) \tag{30}$$

where λ_{seq} (kJ/kg), h_{seq} (kJ/kg) and Q_{seq} (kJ) represent the latent heat and enthalpy of the steam, and the energy requirements of the sequence, respectively. T_{F} (K) is the flame temperature and T_{S} (K) is the stack temperature.

3.5 Control strategy

As is well known, two kinds of disturbances (feed flow rates and compositions) always take place in the real plant operation causing the deviation of the operating conditions from their desired conditions. Hence, control scheme of the proposed process should be investigated to ensure on-specification products. It is important that the obtained products purities are achieved at the specified values (otherwise, the products cannot be sold). However, composition measurements are expensive and often unreliable, being also characterized by large time delays. Thus, the solution is employing the inferential control: as there is a direct relationship between boiling point and

composition, controlling temperatures in the distillation column by manipulating other variables (*e.g.*, reboiler duty or reflux ratio). Sensitivity analysis and singular value decomposition (SVD) criteria for determining the temperature-sensitive stage are proposed by Moore[51] and Luyben[52].

In this work, **n** stages of the column are assumed. Therefore, the steady-state gain matrix, **K**, has **n** rows and **m** columns (**m** represents the number of manipulated variables) and it can be obtained *via* the Eq. 31. Gain matrix **K** is then decomposed to obtained the **U** vector *via* the SVD function of Matlab in Eq. 32.[51]

$$K = \frac{\Delta C_V}{\Delta M_V} \tag{31}$$

$$K = U \sum V^T \tag{32}$$

where the temperature varying in stages is $\mathbf{\Delta C_V}$ and the change of manipulated variables is represented as $\mathbf{\Delta M_V}$. Two orthonormal matrices are denoted as **U** and **V**.

4. Results and discussion

Ternary azeotropic mixtures EtAC/EtOH/water are generated in the production process of *n*-butanol synthesis from ethanol.[3] The flow rates of the feed mixtures are 1124.0 kmol/h with a composition of 53.81 mol% EtAC, 27.59 mol% EtOH, 18.58 mol% water, trace acetaldehyde (AA) and *n*-butanol (BuOH) (*i.e.*, 0.01 mol% AA and BuOH). UNIQUAC model is determined to describe the vapor-liquid equilibrium of this multi-azeotrope complex system while binary interaction parameters of the separation system are listed in Table S2.[3]

4.1 Entrainer determination

Two candidate entrainers DMSO and PG are preliminary screened from three entrainers (DMSO, PG, and EG) based on the key physical properties as shown in Table S3. According to feasibility criteria proposed in our previous studies[18, 53], the separation efficiency of entrainer is

further evaluated by the comparison of the intersection location of iso- and uni- volatility curve and entrainer-one target component side edge of the triangle. The small distance of the intersection to target component indicate that the less the amount of entrainer is needed, and the low operational and capital costs. In order to find the best entrainer in two candidates, the iso- and uni- volatility lines at 100 kPa for six ternary systems (*i.e.*, EtAC/EtOH/DMSO, EtAC/EtOH/PG, EtOH/water/DMSO, EtOH/water/PG, EtAC/water/DMSO and EtAC/water/PG) are introduced and shown in Figure 5.

From the comparison of the intersection between one target component (*i.e.*, EtAC, EtOH and EtAC in Figure 5a–b, 5c–d and 5e–f, respectively) and iso-volatility, the results illustrate that the entrainer DMSO is better than the entrainer PG. Besides, the intersection between one target component and uni-volatility of DMSO is also small than that of PG. In summary, the ability of enhancing relative volatility of three azeotropes using entrainer DMSO is superior to that using entrainer PG. Hence, the entrainer DMSO is finally determined to be used in the separation of azeotropic mixtures EtAC/EtOH/water.

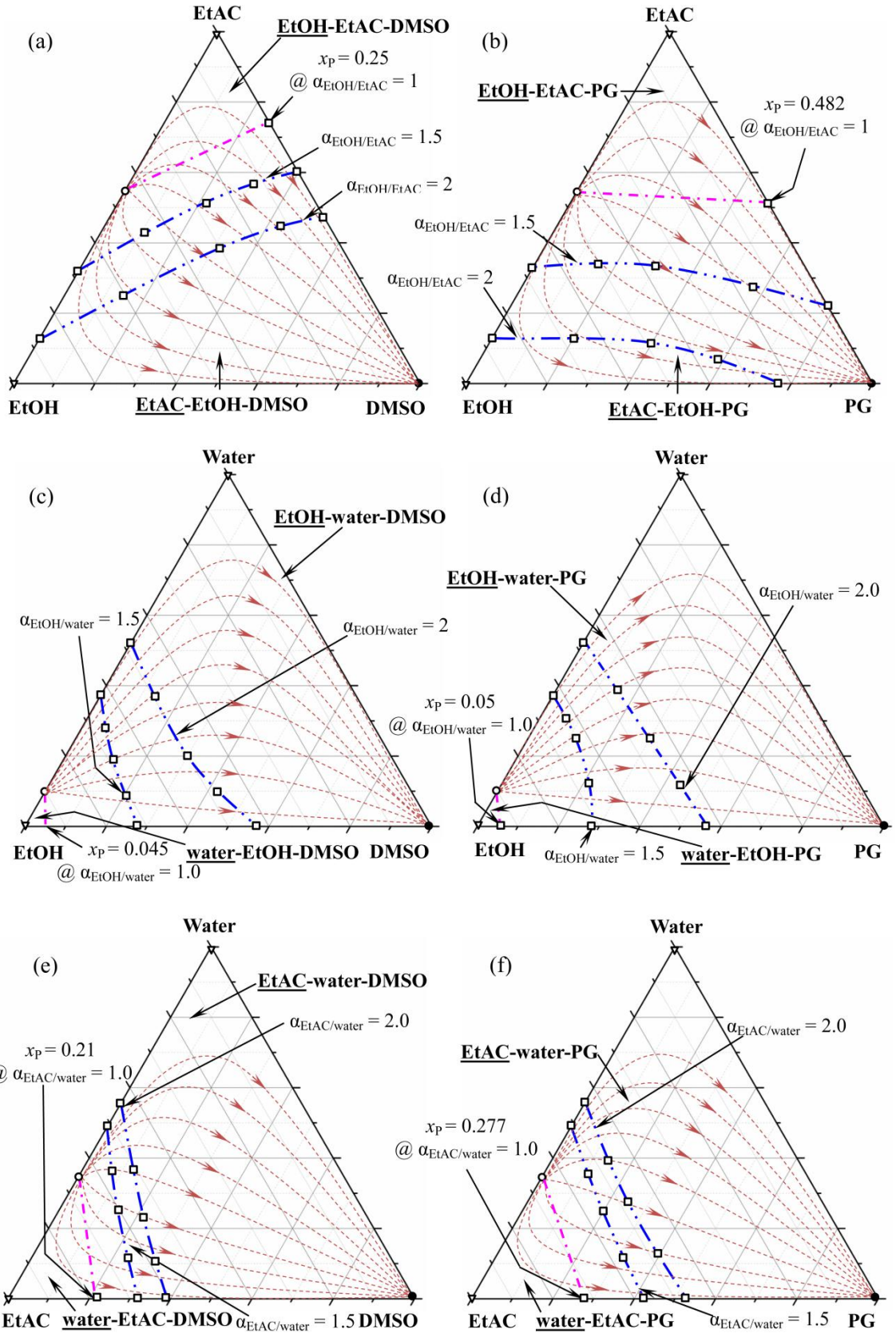

Figure 5. Iso- and uni-volatility lines at 100 kPa for (a), (b) EtOH/EtAC, (c), (d) EtOH/water and (d), (f) EtAC/water using entrainer DMSO and PG, respectively

4.2 Conceptual design

To conceptually design the TCED process, the operating pressure and possible product volatility orders can be obtained *via* the analysis of RCMs and uni-volatility lines for three ternary systems EtAC/EtOH/DMSO, EtOH/water/DMSO and EtAC/water/DMSO, respectively. The EtAC-EtOH-DMSO represents the component EtAC is the first distillate product (see Figure 6a). Similar observations can be obtained from parts of Figure 6b–c.

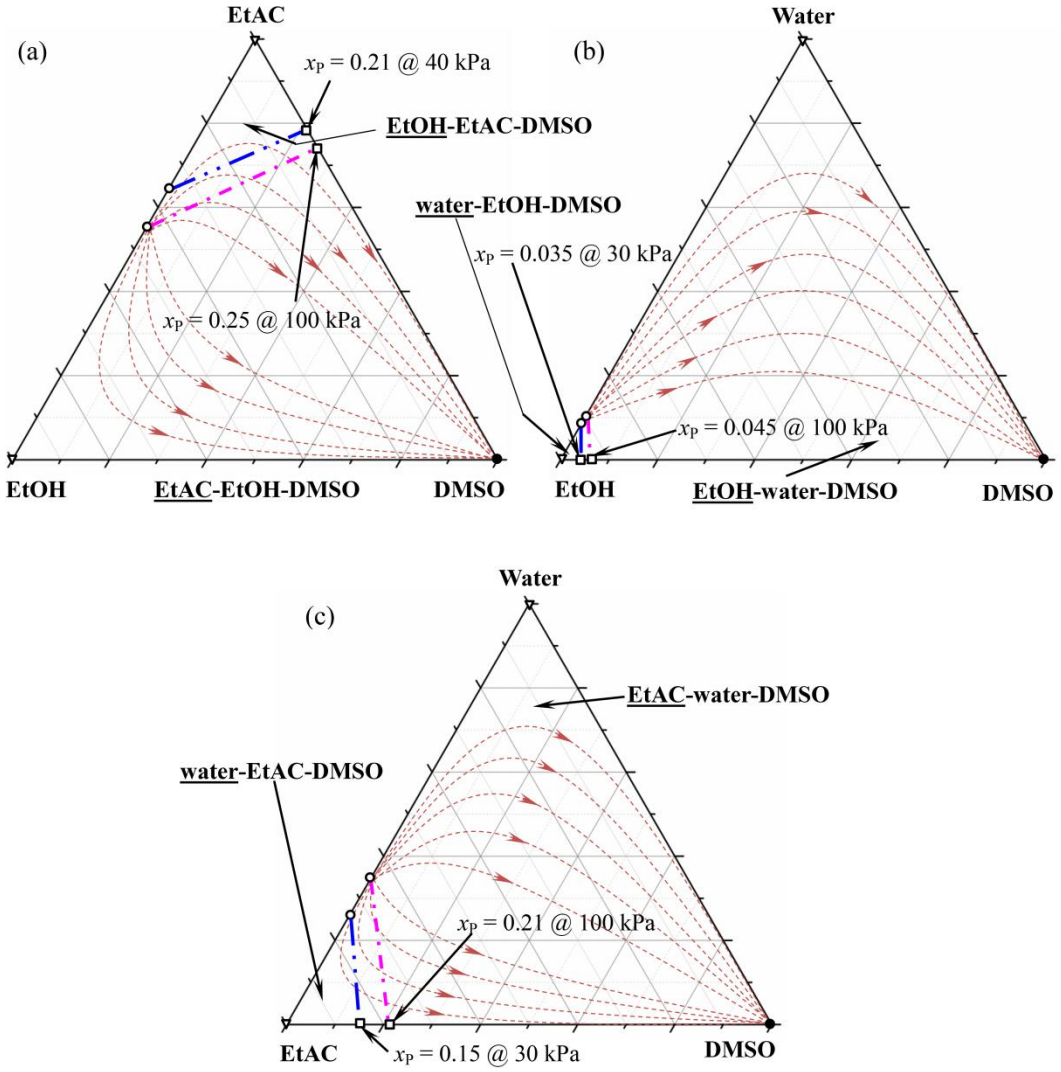

Figure 6. RCMs, uni-volatility lines, and volatility orders of ternary mixtures for (a) EtAC/EtOH/DMSO, (b) EtOH/water/DMSO and (c) EtAC/water/DMSO

The operational pressures of three columns are determined by two key criteria: (1) a pressure increases the volatility of azeotropic mixtures[18] and (2) a pressure permits the use of cooling water

in the condenser[29]. Pressures of 40, 30 and 15 kPa are determined for the columns EDC1, EDC2 and ERC to permit the use of cooling water in the condenser. Furthermore, the values of x_P at 40, 30 and 15 kPa are less than those of at 100 kPa, resulting in the less entrainer are needed for the separation process.

4.3 Optimization results

Optimization results of the proposed TCED process including 213 designs (see Table S4) are eventually obtained *via* the **CPOM**. The global optimization model, **CPOM**, is used and the computation is carried out on the desktop with Intel Core i5-7400 CPU@3.00GHZ, 8 GB memory (about 2 h).

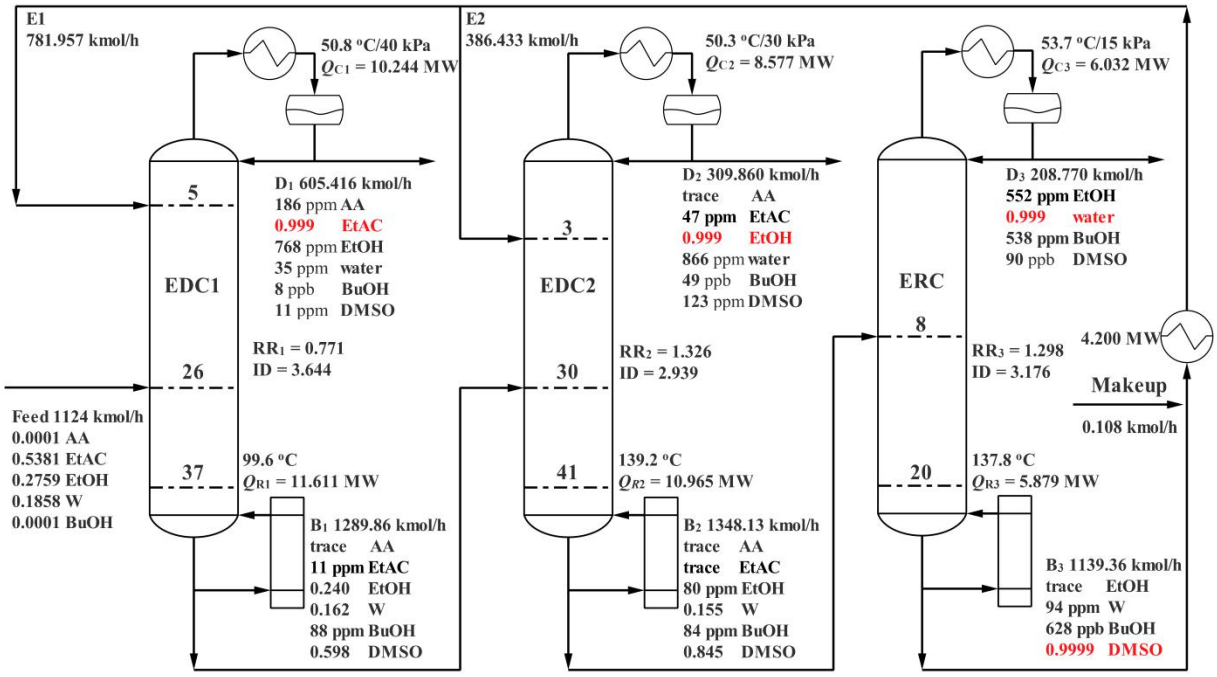

Figure 7. Optimal TCED process for separating EtAC/EtOH/water system using entrainer DMSO

The proposed optimal TCED process for the separation of ternary azeotropic system EtAC/EtOH/water with DMSO as entrainer is presented in Figure 7. The optimal total numbers of stage for the three columns are 38, 42 and 21, respectively. The fresh feed and entrainer stream are respectively fed to 5th and 26th stages in the column EDC1. The EtAC production with high purity

99.90 mol% is obtained at the top of the EDC1. The bottom stream (B_1) and entrainer (E_2) are then respectively fed to 3th and 30th stages of the column EDC2 and the EtOH of 99.90 mol% is distillated. Finally, the bottom stream of EDC2 is fed to the ERC to distillate the 99.9 mol% water and recover 99.99 mol% DMSO.

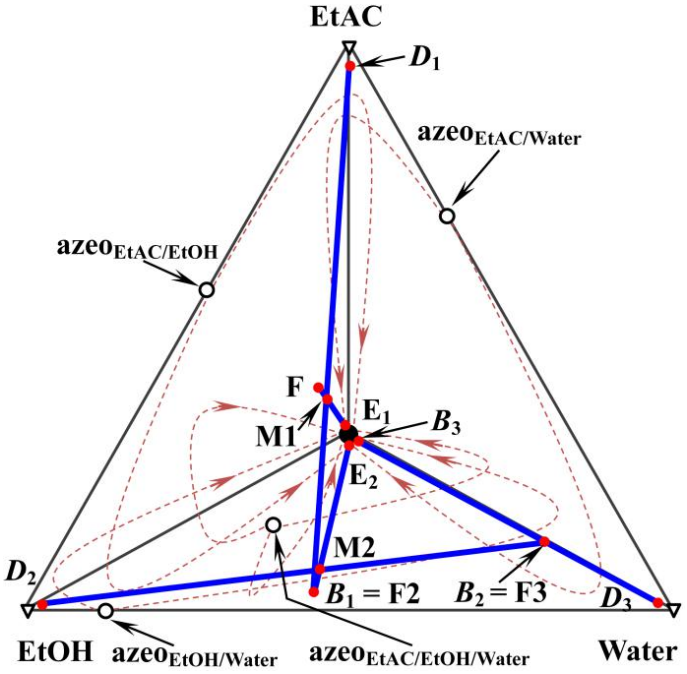

Figure 8. Material balance lines for separating azeotropic system EtAC/EtOH/W using TCED

Figure 8 gives the material balance lines of the optimal TCED process. The fresh feed denoted as F is mixed with an entrainer stream denoted as E_1 (DMSO) as an input (M_1) for the column EDC1. The mixture stream M_1 is separated into distillate product denoted as D_1 (EtAC) and bottom non-product stream B_1. Stream B_1 is fed to the column EDC2 to obtain EtOH with 99.90 mol% at overhead D_2 stream and a mixture B_2 (water and DMSO) is obtained at the bottom. The mixture B_2 is then sent into the column EDC, high purity of DMSO (E_2) is obtained at the bottom stream and then is recycled to the columns EDC1 and EDC2.

Table 1. Comparison of the optimal design among FCED and TCED processes

	Existing FCED	Proposed TCED
N_{T1}	40	37

N_{T2}	20	42
N_{T3}	40	21
N_{T4}	20	-
F_{E1} (kmol/h)	987.000	781.957
F_{E2} (kmol/h)	707.600	386.433
Q_{C1} (MW)	9.270	10.244
Q_{R1} (MW)	11.440	11.611
Q_{C2} (MW)	7.680	8.577
Q_{R2} (MW)	9.290	10.965
Q_{C3} (MW)	3.860	6.032
Q_{R3} (MW)	6.520	5.879
Q_{C4} (MW)	5.240	-
Q_{R4} (MW)	5.920	-
Cost of vacuum system ($\times 10^6$ \$/y)	0.256	0.287
TOC ($\times 10^6$ \$/y)	3.687	3.060
TCC ($\times 10^6$ \$)	7.418	6.693
TAC ($\times 10^6$ \$)	6.160	5.291
Saving (%)	0.00	14.11

Table 1 summarizes the computational results of TOC, TCC and TAC of the two processes. The TAC of the process TCED is by 14.11% lower than that of the referenced process FCED mainly attributing to lower TOC and TCC.

Table 2 gives a comparison of exergy loss and CO_2 emissions among the processes of TCED and FCED.

Table 2. Results of CO_2 emissions and exergy loss of the two separation configurations

	Existing FCED	Proposed TCED
Q_{R1} (MW)	11.440	11.611
Q_{R2} (MW)	9.290	10.965
Q_{R3} (MW)	6.520	5.879
Q_{R4} (MW)	5.920	-
Q_{total} (MW)	33.170	28.455
Total exergy loss (MW)	4.472	3.789
CO_2 emissions (t/h)	11.213	9.619

The *El* and CO_2 emissions for the proposed TCED process are more efficient and environmentally-friendly with 15.23% and 14.22% savings compared to the existing FCED process. In summary, the proposed TCED process is not only economical but also environmental-friendly

and lower exergy loss.

4.4 Dynamic results

4.4.1 Determination of temperature control point

For the design of control scheme, locations of temperature–sensitive stages in distillation columns are first determined. Open-loop sensitivity analysis results on temperature profiles of three columns are displayed in Figure 9a–f. In this process, a very small ±0.1% step to each manipulating variable is given while the other manipulating variables are fixed.

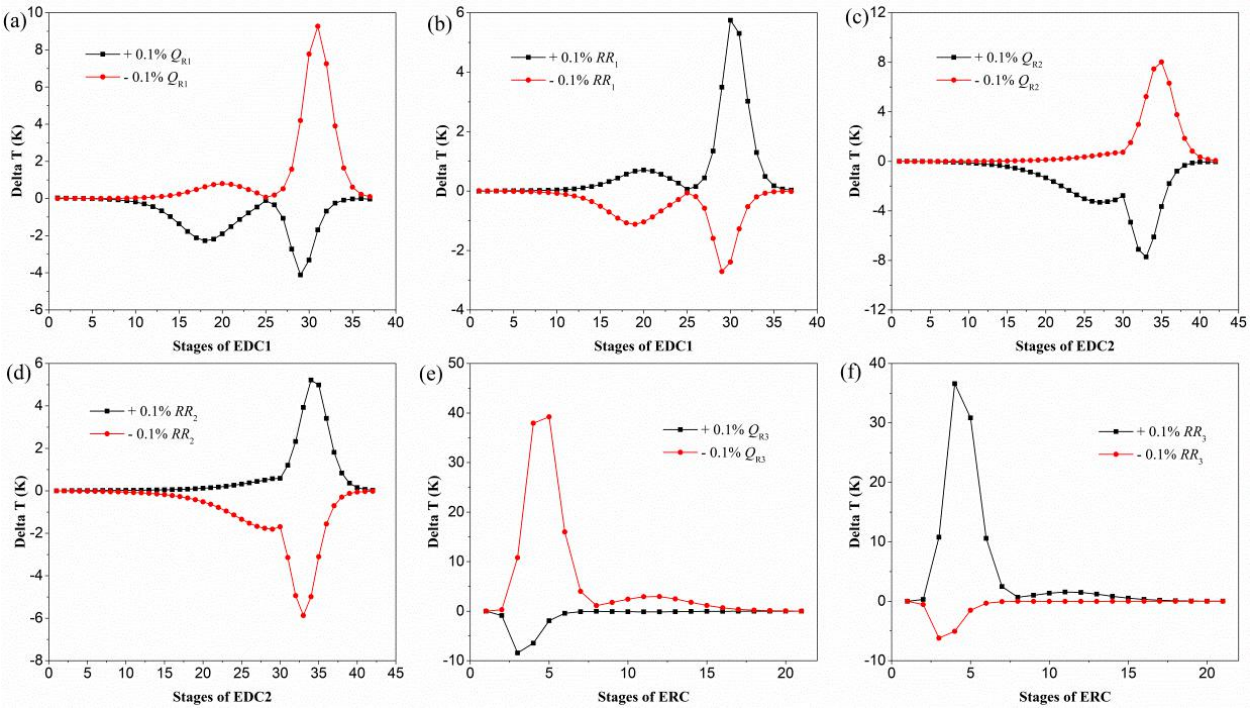

Figure 9. Open-loop sensitivity analysis results on temperature profiles in (a), (b) EDC1, (c), (d) EDC2 and (e), (f) ERC by varying ±0.1% reboiler duty and reflux ratio

The temperatures on stage 30, 33 and 4 (*i.e.*, $T_{30\text{-EDC1}}$, $T_{33\text{-EDC2}}$ and $T_{4\text{-ERC}}$) have large peaks that can be determined as a temperature-sensitive stage to maintain product purities from.

Table 3. Gain and integral time for tray temperature controllers using Tyreus–Luyben tuning method in three control strategies CS1, CS2 and CS3

controllers	tuning parameters	controller action	CS1	CS2	CS3
TC1	K_C	reverse	0.638	0.638	0.609
	τ_I [min]		22.440	22.440	23.760
TC2	K_C	reverse	0.819	0.819	0.822

	τ_I [min]		21.120	21.120	19.800
TC3	K_C	reverse	0.368	0.368	0.357
	τ_I [min]		19.800	19.800	18.480
TC4	K_C	reverse	0.210	0.210	0.210
	τ_I [min]		9.240	9.240	9.240
TC5	K_C	direct	-	1.087	1.087
	τ_I [min]		-	29.040	29.040

The tuning parameters integral time (τ_I) and gains (K_C) of temperature controllers are given in Table 3, which are obtained *via* the Tyreus–Luyben approach (see in Eqs. 33–34).[54] Disturbances of flow rate and composition are interposed at t = 1 h to assess the dynamic performances of the proposed TCED scheme, which is illustrated as below.

$$K_C = K_U / 3.2 \tag{33}$$

$$\tau_I = 2.2P_U \tag{34}$$

4.4.2 Basis control strategy with fixed reflux ratio (CS1)

Based on the control scheme of the conventional extractive distillation system and the suggestions of Zhang et al.[55], the basic control scheme of the TCED is proposed. Figure 10 illustrates the basic control scheme for the separation of EtAC/EtOH/water using TCED. The detailed control loops are summarized as below.

(1) Flowrate of fresh feed is maintained by controlling the valve opening (reverse acting);

(2) Operating pressures of all columns are controlled through manipulating the condenser duty (reverse acting);

(3) Distillate rates are used to control the levels of reflux drum (direct acting);

(4) Levels of sump in the EDC1 and EDC2 are maintained by adjusting the product rate of bottoms (direct acting);

(5) Sump level in the ERC is controlled by adjusting the makeup flow rate (reverse acting);

(6) Distillate and reflux rates are proportionated;

(7) The entrainer flow rate of the EDC2-to-flow rate of EDC1 bottom is fixed;

(8) Total flow rates of entrainer and feed are proportionated;

(9) The temperature of recycled entrainer is controlled at 50 °C *via* the manipulation of the condenser duty (reverse acting);

(10) Reboiler duties are manipulated through the temperature of the corresponding temperature-sensitive stage (reverse acting).

K_C of 0.5 and τ_I of 0.3 min are suggested for feed controllers (*i.e.*, FC and FC_{tot}).[13, 14] K_C and τ_I of all pressure controllers (*i.e.*, PC1, PC2 and PC3) are set as default values 20 and 12, respectively and Gain K_C = 2 and a large integral time τ_I = 9999 min are given in all level controllers (*i.e.*, LC1, LC2, LC3, LC4, LC5 and LC6).[37, 56] In addition, dead time with 1 min is inserted to all temperature control loops (*i.e.*, TC1, TC2, TC3 and TC4).[55-58]

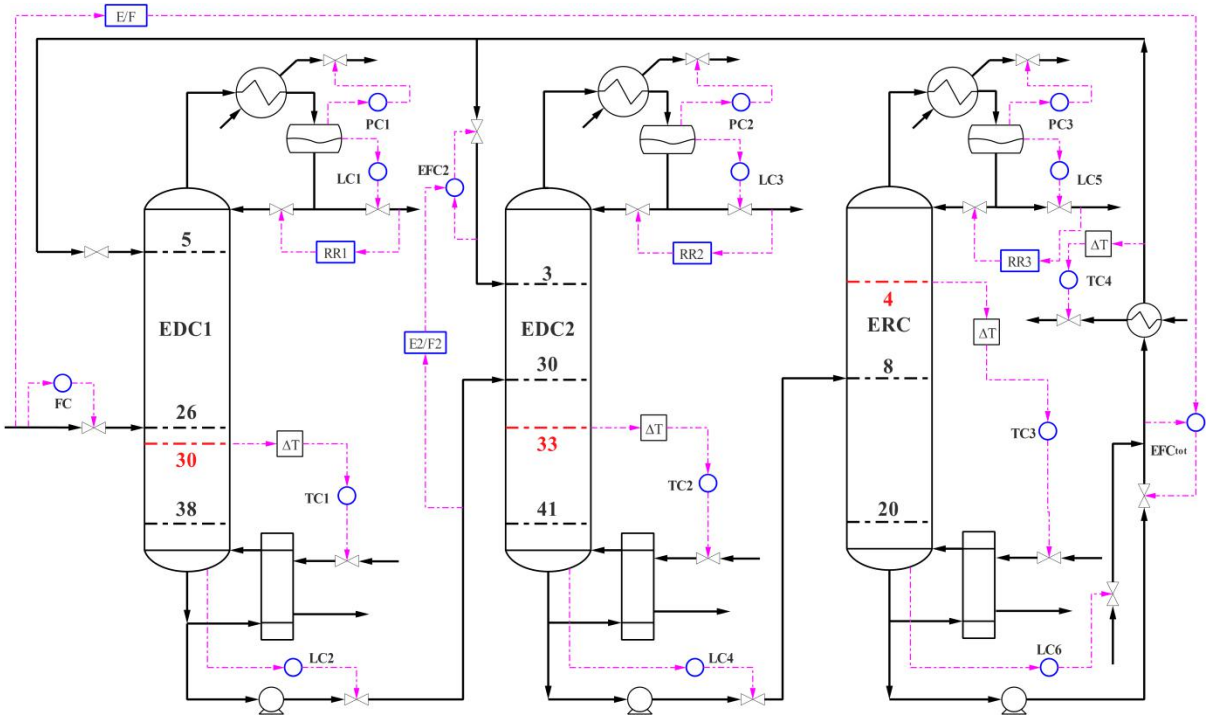

Figure 10. Basic control structure with fixed reflux ratio for separating EtAC/EtOH/water using TCED

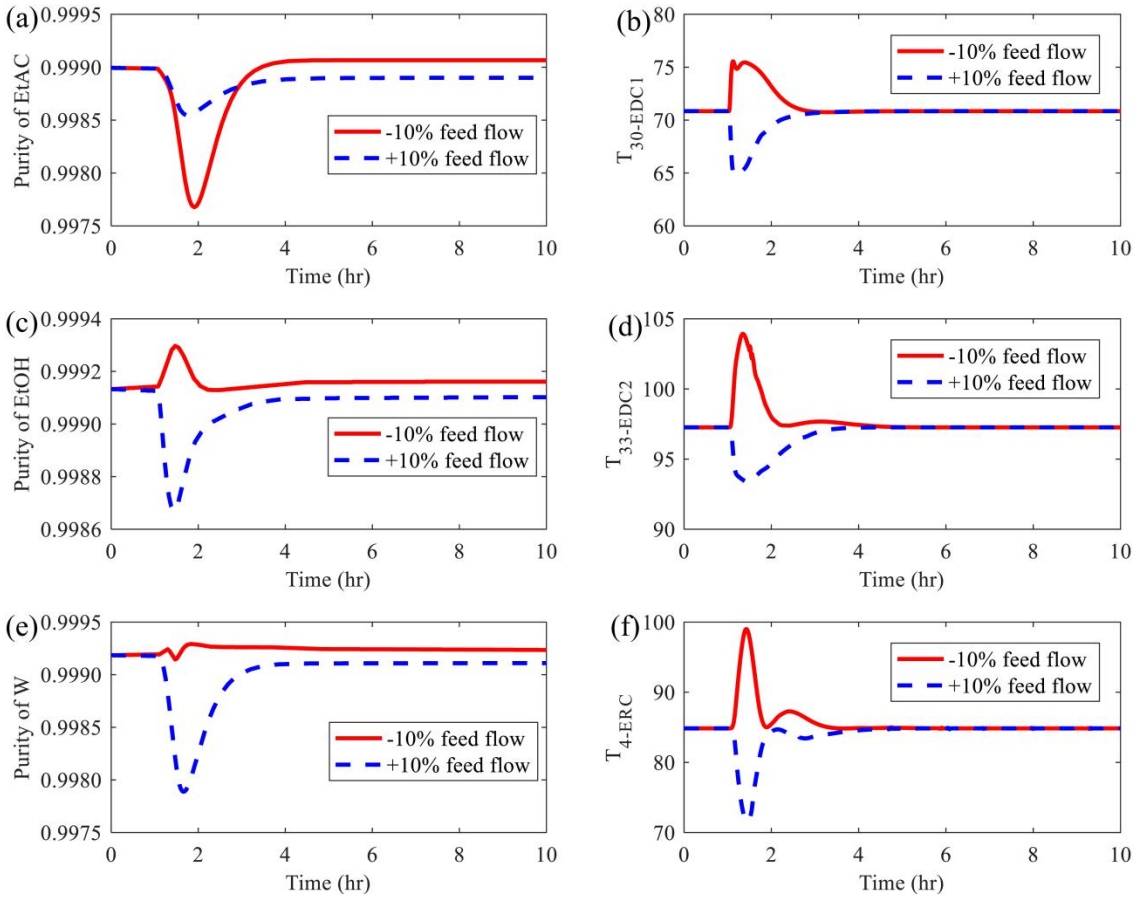

Figure 11. Dynamic responses of CS1 under ±10% feed flow rate disturbances

Figure 11 illustrates the dynamic performances of the basic control strategy for the TCED with DMSO as an entrainer by interposing ± 10% feed flow rates disturbances. TCED process could reach at a new stable condition with 4 h. At present, the products purities of EtAC, EtOH and water are respectively 99.9066, 99.9161 and 99.9235 mol% by decreasing 10% feed flow rates while the product purities are respectively 99.8900, 99.9102 and 99.9110 mol% by increasing 10% feed flow rates. Hence, products purities of EtAC, EtOH and water are maintained close to their specified purities.

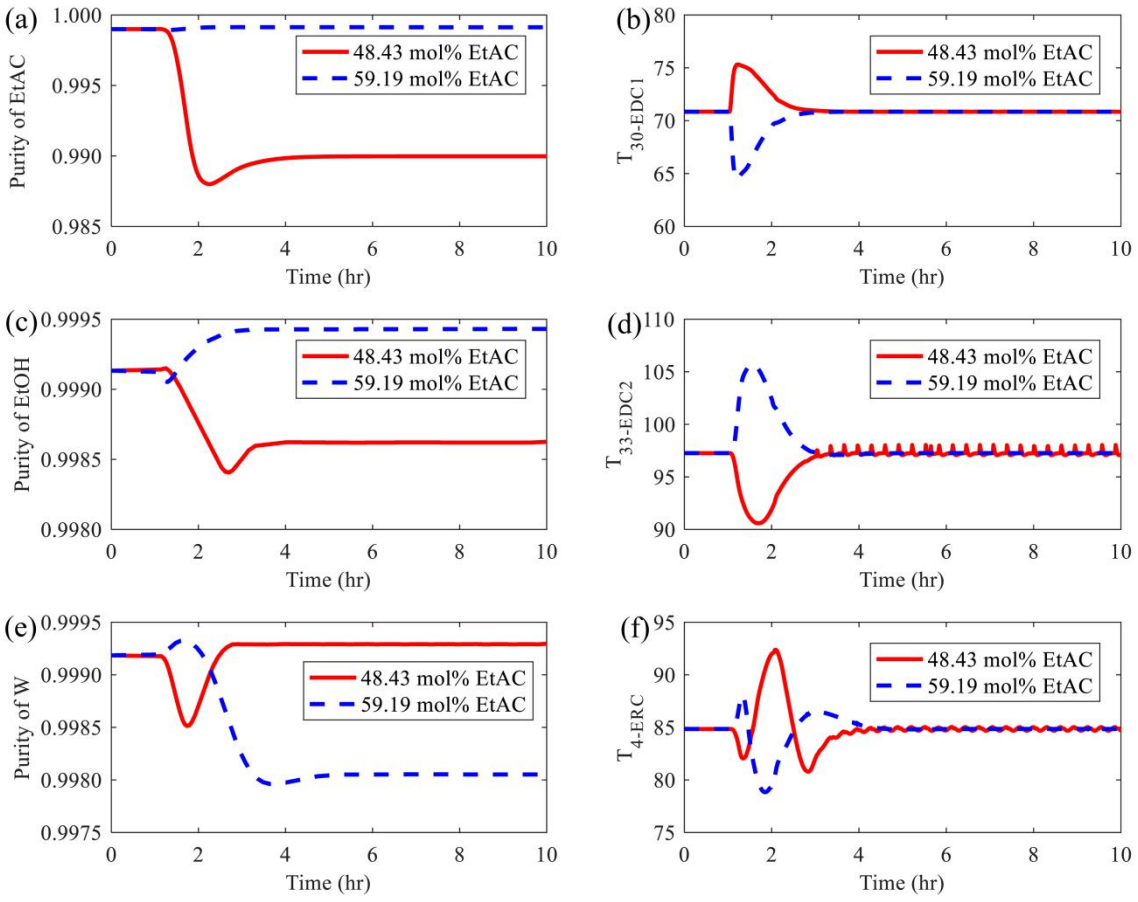

Figure 12. Dynamic responses of CS1 under ±10% feed composition disturbances

The dynamic performances of the basic control strategy for the TCED are illustrated in Figure 12. The purities of EtAC, EtOH and water are respectively 99.9126, 99.9431 and 99.8052 mol% close to their specified values (+10% feed composition disturbance) when the new steady-state arrives. The decreasing 10% feed composition disturbance (*i.e.*, 48.73 mol% EtAC) is added, EtOH and water purities are controlled to their specified points. Of note is that purity of EtAC could not be effectively controlled (from 99.9000 mol% to 98.9977 mol%). Consequently, the temperature control structure could not efficiently manage the feed disturbances.

4.4.3 Dual temperature control strategy (CS2)

To overcome the issues of large vibration in the product purity of EtAC facing -10% composition disturbance (*i.e.*, red solid line in Figure 12a), another temperature-sensitive stage is

then selected to manipulate the reflux ratio of the column EDC1. However, there are existing two similar peaks on 20th and 30th stages, which are both sensitive to the changes of Q_{R1} and RR_1 (see in Figure 9a–b). Following the suggestion of Moore[51] and Luyben[52], the SVD method is used to select positions of control point for multi-variable system by decomposing the steady-state gain matrix.

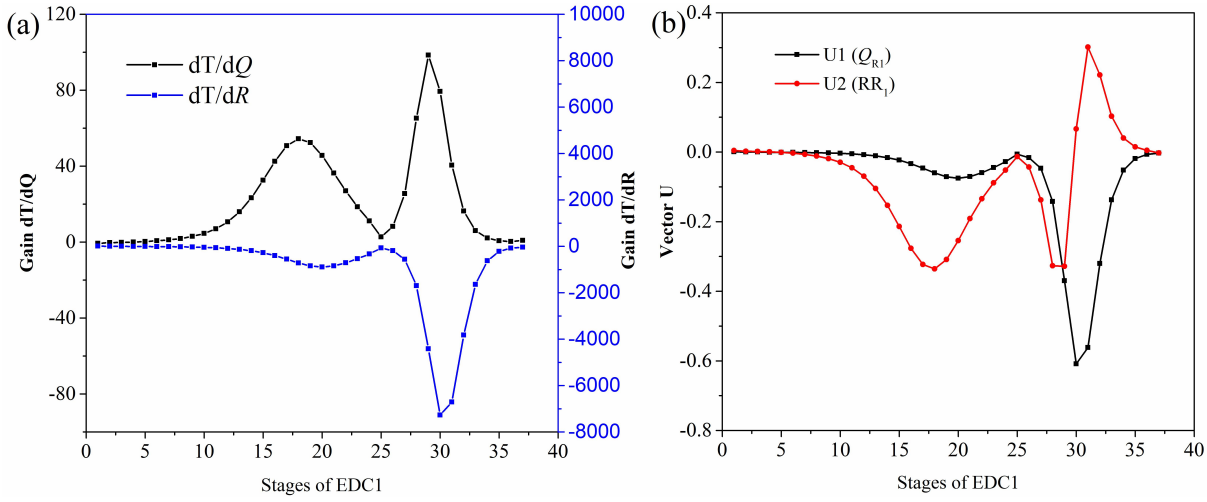

Figure 13. (a) steady-state gains and (b) SVD analysis results

Figure 13a–b demonstrates the results of steady-state gains and SVD for the changes of RR_1 and Q_{R1}, respectively. The temperature on 20th stage ($T_{20\text{-EDC1}}$) of EDC1 has large **U2** vector values for the change of RR_1 and could be used to handle top product purity by adjusting RR_1. The temperature on 30th stage ($T_{30\text{-EDC1}}$) of C1 gives the large **U1** vector values to the change of Q_{R1} and should be selected to adjust Q_{R1}. Following that, the dual temperature control scheme of the TCED is designed and shown in Figure 14. Two temperature control loops are added, in which temperatures of 20th and 30th stages in the EDC1 are controlled through adjusting the RR_1 and Q_{R1}, respectively. It should be noted that the controller action of the TC5 is direct (*i.e.*, increasing reflux ratio as the temperature increasing).

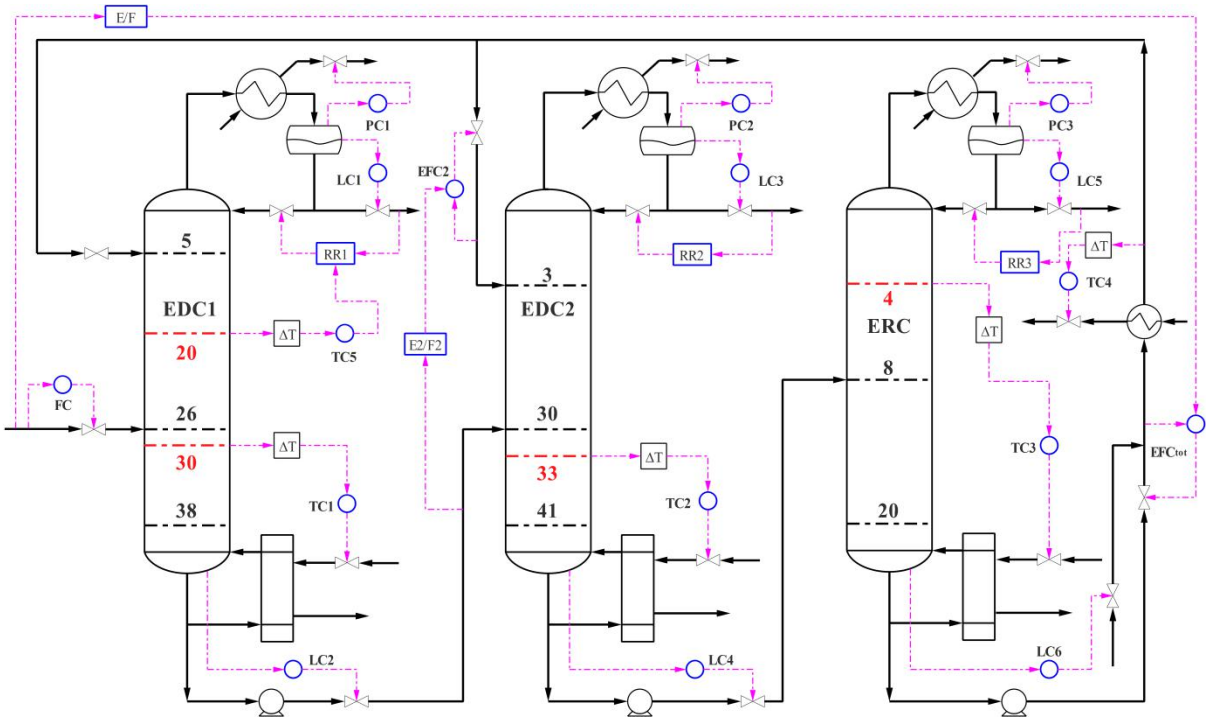

Figure 14. Dual temperature control strategy for the proposed TCED process

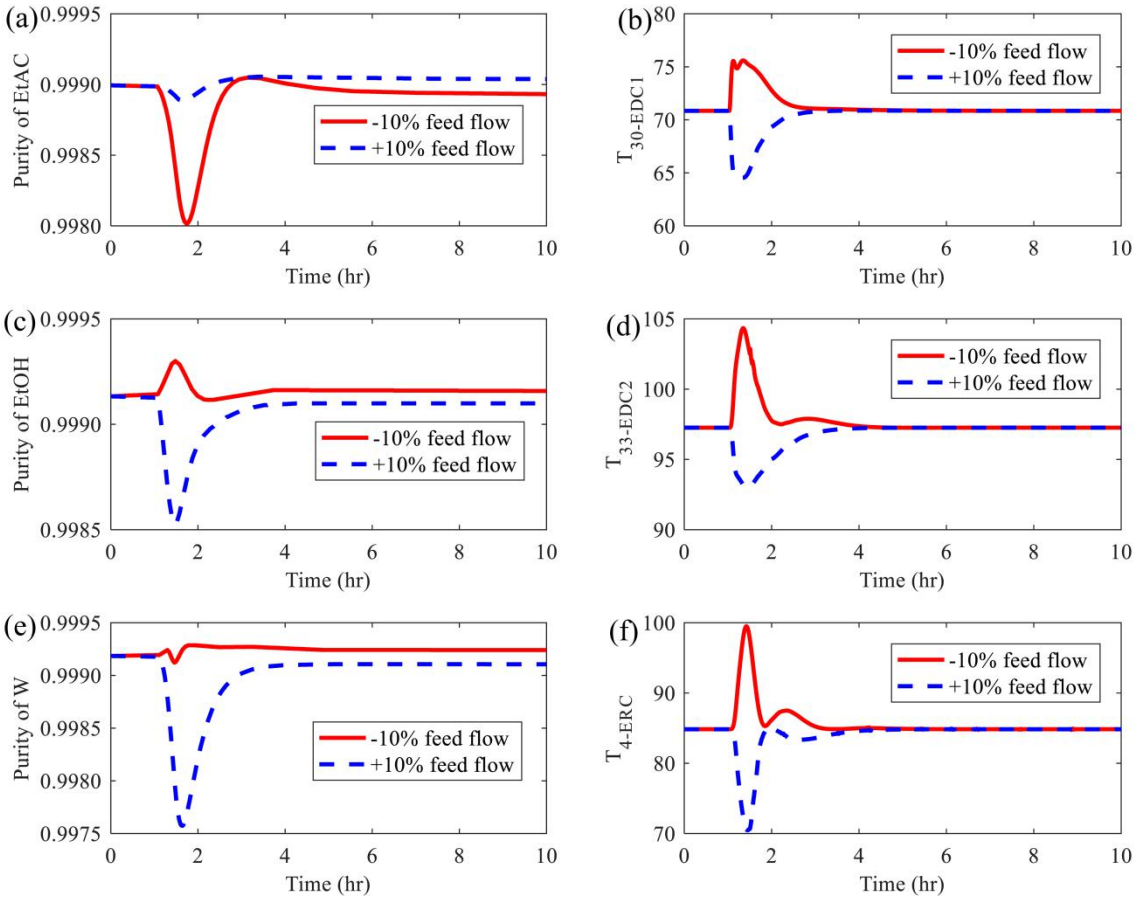

Figure 15. Dynamic responses of CS2 under ±10% feed flow rate disturbances

The dynamic performances with ±10% feed flow rate disturbances are demonstrated in Figure

15. The products purities of EtAC, EtOH and water are gotten back to their specified values (about 2 h) when the flowrate is increased to 1236.4 kmol/h and is decreased to 1011.6 kmol/h. In summary, the products purities could be controlled to specified values facing the disturbances of feed flowrate.

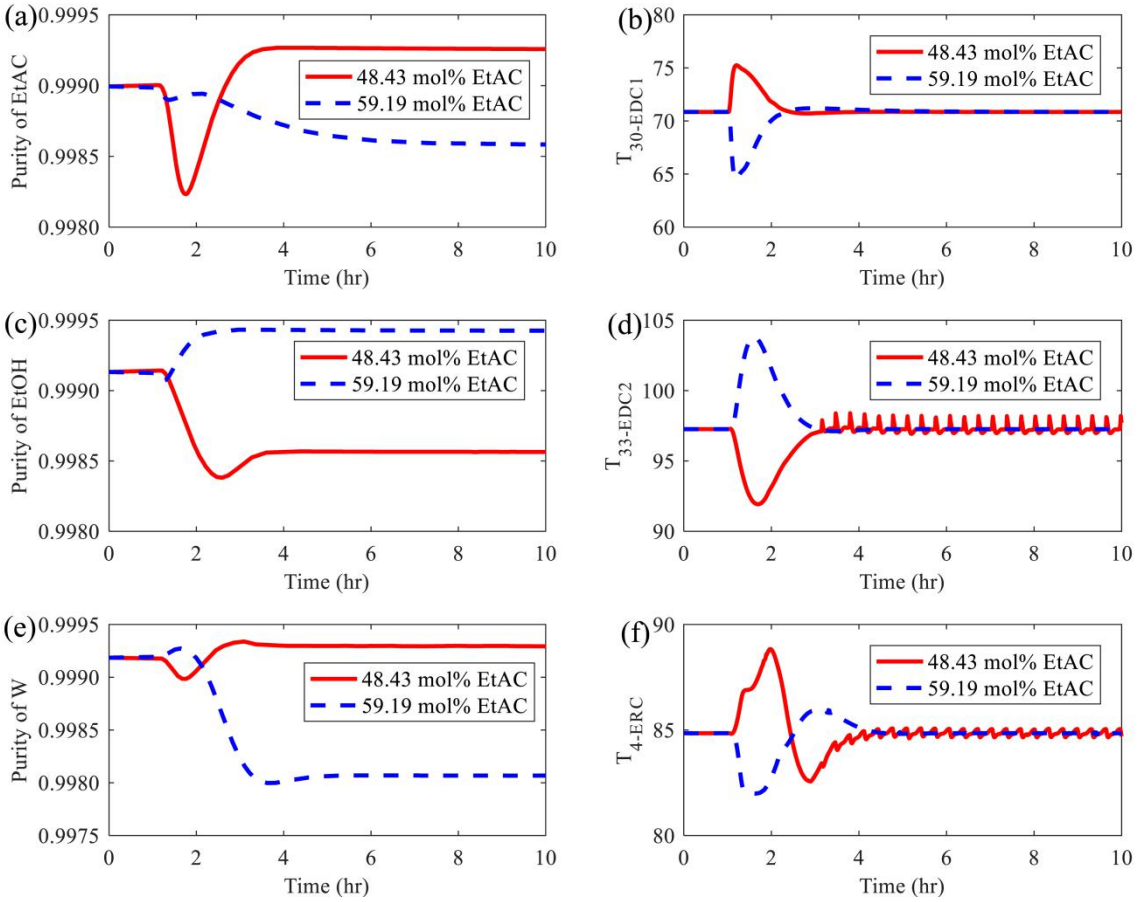

Figure 16. Dynamic responses of CS2 under ±10% feed composition disturbances

Dynamic performances of the dual temperature control scheme by adding ±10% feed disturbances of composition are shown in Figure 16. The products purities of EtAC, EtOH and water could be gotten back to their specified values (3h). For the decreasing 10% feed composition, the products purities of EtAC, EtOH and water are 99.9263, 99.8556 and 99.9304 mol%, respectively. For increasing 10% feed composition, they are 99.8584, 99.9427 and 99.8067 mol%. In summary, dual temperature control scheme has advantage for the same disturbances. Of note is

that the large of peak transient deviations and offsets in the CS2 are also existed. Hence, a more robust feedforward control strategy is studied in the following section.

4.4.4 Improved Q_R/F control structure (CS3)

To improve the disturbance rejection capability of the dual temperature control scheme CS2, feedforward structure Q_R/F is proposed and illustrated in Figure 17. Three multipliers (Q_{R1}/F_1, Q_{R2}/F_2 and Q_{R3}/F_3) are added in the improved control structure CS3.

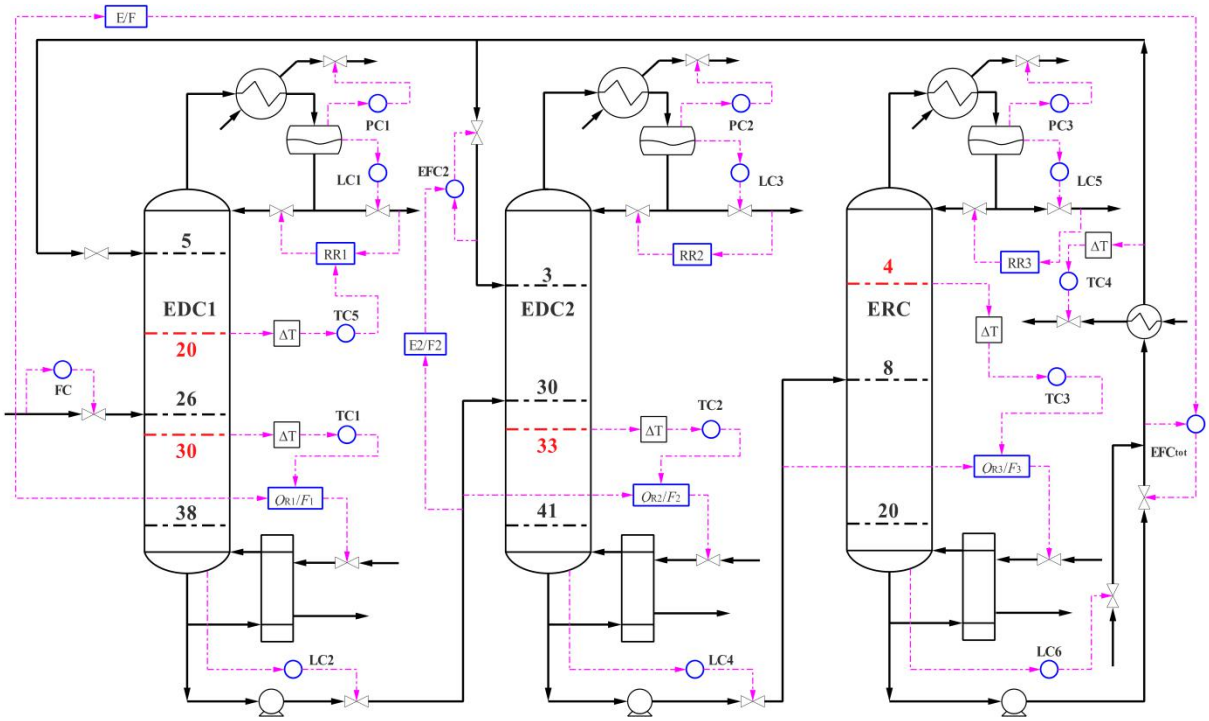

Figure 17. Improved Q_R/F control structure for the proposed TCED process

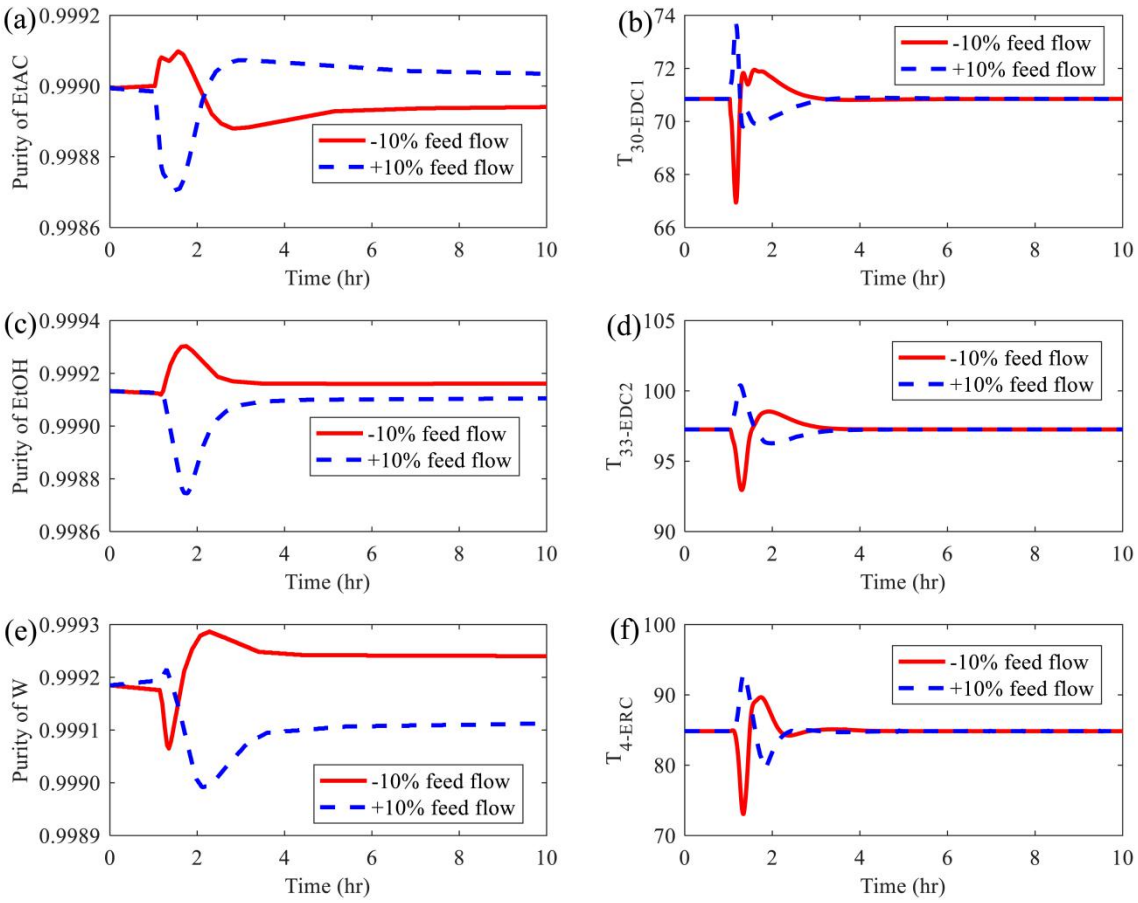

Figure 18. Dynamic responses of CS3 under ±10% feed flow rate disturbances

Dynamic performances of the proposed robust control scheme CS3 are illustrated in Figure 18. EtAC purities of distillate in the EDC1 are 99.9035 and 99.8941 mol%, respectively, which are close to their specified value (*i.e.*, 99.9000 mol%). Dynamics performance of EtOH and water could be seen from Figure 18c−f.

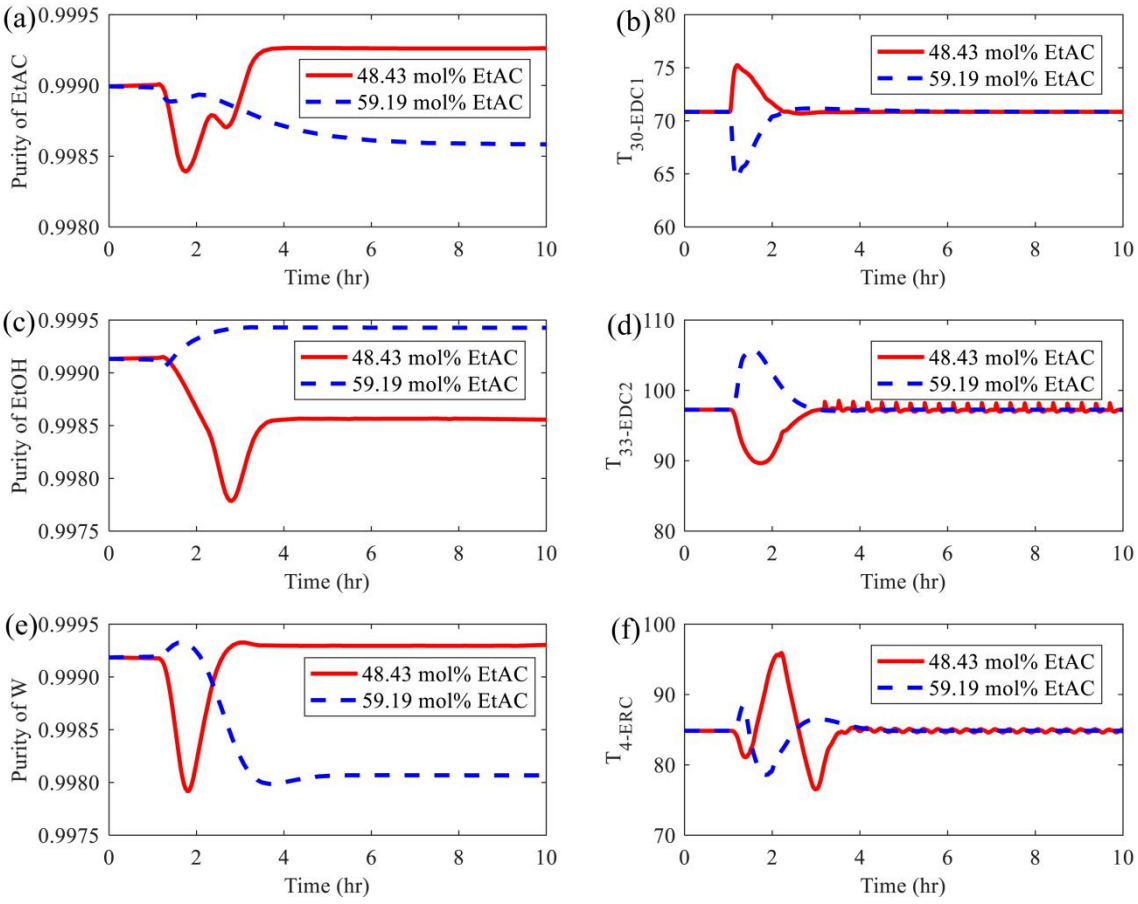

Figure 19. Dynamic responses of CS3 under ±10% feed composition disturbances

Feed disturbances of compositions (*i.e.*, 59.19 and 48.43 mol% EtAC) are introduced to assess the dynamic performance of the proposed control scheme CS3 (see Figure 19a−f). The product purities could be quickly gotten back to their desired values (*i.e.*, 3h) under fresh feed composition disturbances.

4.4.5 Comparison of three control structures

In order to clearly observe the dynamic performances of three control schemes more intuitively, comparison of dynamic responses between CS1, CS2 and CS3 under ±10% feed flow rates and composition disturbances are demonstrated in Figures 20 and 21.

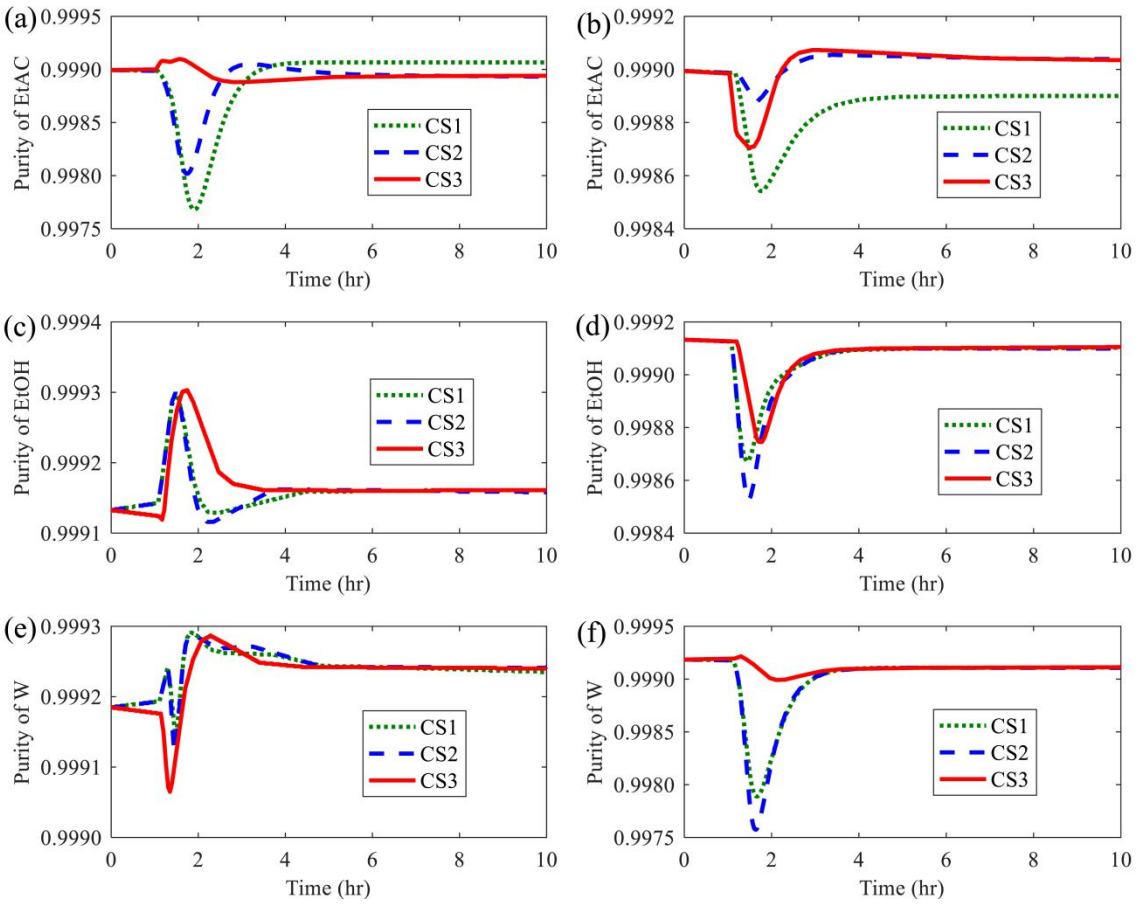

Figure 20. Comparison of dynamic responses between CS1, CS2 and CS3 under ±10% feed flow rate disturbances

Figure 20 illustrates the comparison of dynamic responses between CS1, CS2 and CS3 under ±10% feed flow rates disturbances. Compared to the scheme CS1, CS2 and CS3 exhibit similar dynamic responses with small offsets while rejecting the disturbances in -10% feed flow rate (see Figure 20a, c and e). At the same time, small offsets of the purities for EtOH and water has also exhibiting in control strategies CS2 and CS3 (see Figure 20d and f). In contrast, the dynamic responses of product purities EtAC in scheme CS3 have relatively larger offsets than those in CS2 scheme (see Figure 20b) when the +10% feed flow rate disturbances are introduced at t = 1 h.

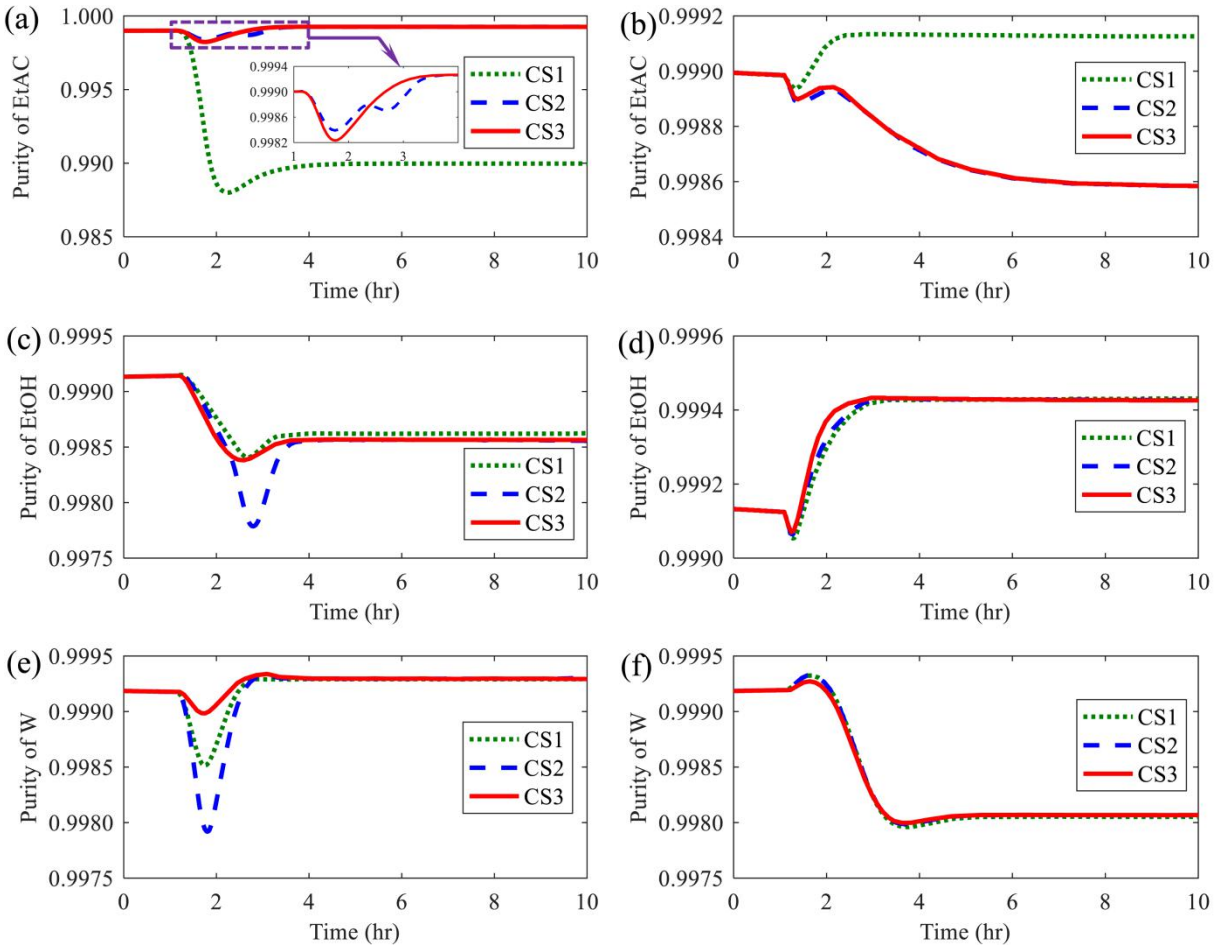

Figure 21. Comparison of dynamic responses between CS1, CS2 and CS3 under ±10% feed composition disturbances

Figure 21 shows the comparison of dynamic performances between CS1, CS2 and CS3 under ±10% feed composition disturbances. Compared to the basic control scheme CS1, improved control strategies CS2 and CS3 display similar dynamic performances with small offsets while rejecting the disturbances in -10% feed composition (see Figure 21a, c and e). Meanwhile, small offsets of the purities of EtOH and water has also exhibiting in CS2 and CS3 (see Figure 21d and f). In contrast, the dynamic responses of EtAC product purities in CS2 and CS3 schemes have relatively larger offsets than those in CS1 scheme (see Figure 21b) when the +10% feed composition disturbances are introduced at t = 1 h. To obtain the higher purity of EtAC, the temperature of extractive and rectifying sections should be increased compared with the specified values for the +10% feed

composition disturbances (see Figure 21b). However, in the control structure CS1, the temperatures of stripping section in column EDC1 could be maintained at their specified values via the temperature controller TC1 while these of extractive and rectifying sections could not be well controlled (*i.e.*, greater than the specified value of temperature resulting in higher EtAC concentration). In both control schemes CS2 and CS3, the temperatures of extractive and rectifying sections could be controlled (*i.e.*, equal to the specified value) through two temperature controllers TC1 and TC5. Therefore, the final EtAC concentration in the distillate is increasing for CS1 and decreasing for CS2 and CS3 when +10% feed composition disturbances are introduced.

The improved control strategy CS3 with dual temperature and feedforward structures can handle the ±10% feed flow rates and -10% compositions disturbances more effectively than control structures CS1 and CS2. It is worth noting that the purity of EtAC (+10% composition disturbances) could not been well controlled through the improved CS3 because of the temperatures of two controllers TC1 and TC5 are fixed. Therefore, more robust control structure (*e.g.*, temperature difference) will be studied to overcome this issue in the further work.

5. Conclusions

In this work, a systematic procedure for optimal deign and robust control of the EtAC/EtOH/water system separation through the triple-column extractive distillation (TCED) process is proposed. First, the suitable entrainer DMSO is determined *via* the iso- and uni- volatility lines from two candidate entrainers DMSO and PG. Second, the conceptual design of the TCED process is designed by using residue curve maps. The thermodynamic insights results indicate that EtAC, EtOH and water are distillated in three columns, respectively. The proposed process is then optimized based on the global optimization model, **CPOM**, by using TAC as an objective function.

The proposed TCED process is more attractive with lower TAC, CO_2 emissions and exergy loss indicating that the proposed process is much suitable and effective for separating this ternary mixture EtAC/EtOH/water with multi-azeotrope. Finally, an improved control scheme CS3 with dual temperature and feedforward is reported based on the criteria singular value decomposition to control product purities close to their specified values.

Of note is that the proposed systematic method could be widely used for the separation of other ternary multiazeotropes systems methanol/water/tetrahydrofuran and acetonitrile/methanol/water to separate the valuable resources and pursue sustainable development. Furthermore, the improved robust control scheme could provide a theoretical guideline for the control of multi-variable control loops. Besides, the heat integration and thermal coupled processes for separating EtAC/EtOH/water mixture will be further investigated in another work.

Author Information

Corresponding Author

E-mail: shenweifeng@cqu.edu.cn

Notes

The authors declare no competing financial interest.

Acknowledgments

We acknowledge the financial support provided by the National Natural Science Foundation of China (Nos. 21878028, 21606026); the Natural Science Foundation of Chongqing, China (No. CSTC2016JCYJA0474); the Chongqing Innovation Support Program for Returned Overseas Chinese Scholars (No. CX2018048); the Chongqing Social livelihood Technological Innovation and Application Demonstration (No. CSTC2018JSCX-MSYBXX0336).

Helpful comments and suggestions from the paper's reviewers are also gratefully acknowledged.

Supporting Information

The Supporting Information is available free of charge *via* the Internet.

Capital and energy calculation formals are provided in Table S1, binary interaction parameters of the UNIQUAC model for separation system are provided in Table S2, the comparison of the main physical properties between different entrainers is provided in Table S3, and optimization results are provided in Table S4.

Nomenclature

TAC = total annual cost, $\times 10^6$ \$

TOC = total capital cost, $\times 10^6$ \$

TCC = total operating cost, $\times 10^6$ \$

El = exergy loss, MW

E*x* = exergy, MW

SVD = singular value decomposition

SQP = sequence quadratic programming

CPOM = complete process optimization model

FCED = four columns extractive distillation

TCED =triple-column extractive distillation

EtAC = ethyl acetate

EtOH = ethanol

RCMs = residue curve maps

RR = reflux ratio

N_T = total number of stage

N_F = feed location

F_E = entrainer flow rate, kmol/h

D = distillate flow rate, kmol/h

PP = payback period

EDC = extractive distillation column

ERC = entrainer recovery column

K = steady-state gain matrix

$\mathbf{\Delta C_V}$ = change in stage temperatures

$\mathbf{\Delta M_V}$ = step change in manipulated variables

U = orthonormal matrix

V = orthonormal matrix

K_C = gain

τ_I = integral time, min

Q_R/F = reboiler duty-to-feed ratio, GJ/kmol

NHV = the net heating value, kJ/kg

C% = carbon content

α = the molar mass ratio of CO_2 and C

Q_{fuel} = the energy requirements of the fuel, kJ

λ_{seq} = latent heat of the steam, kJ/kg

h_{seq} = enthalpy of the steam, kJ/kg

Q_{seq} = the energy requirements of the sequence, kJ

T_F = the flame temperature, K

T_S = the stack temperature, K

H = enthalpy of the system, kJ/kg

H_0 = enthalpy of the reference, kJ/kg

S = entropy of the system, kJ/kg

S_0 = entropy of the reference, kJ/kg

EG = ethylene glycol

DMSO = dimethyl sulfoxide

PG = propylene glycol

References:

1. Zhang, Q.; Liu, M.; Li, C.; Zeng, A., Heat-integrated pressure-swing distillation process for separating the minimum-boiling azeotrope ethyl-acetate and ethanol. *Sep. Purifi. Technol.* **2017,** *189*, 310-334.

2. Zhang, Q.; Liu, M.; Li, C.; Zeng, A., Design and control of extractive distillation process for separation of the minimum-boiling azeotrope ethyl-acetate and ethanol. *Chem. Eng. Res. Des.* **2018,** *136*, 57-70.

3. Michaels, W.; Zhang, H.; Luyben, W. L.; Baltrusaitis, J., Design of a separation section in an ethanol-to-butanol process. *Biomass Bioenerg.* **2018,** *109*, 231-238.

4. Raeva, V. M.; Sazonova, A. Y., Separation of ternary mixtures by extractive distillation with 1,2-ethandiol and glycerol. *Chem. Eng. Res. Des.* **2015,** *99*, 125-131.

5. Petlyuk, F.; Danilov, R.; Burger, J., A novel method for the search and identification of feasible splits of extractive distillations in ternary mixtures. *Chem. Eng. Res. Des.* **2015,** *99*, 132-148.

6. Garcia, D.; You, F., Systems engineering opportunities for agricultural and organic waste management in the food–water–energy nexus. *Curr. Opin. Chem. Eng.* **2017,** *18*, 23-31.

7. Prayoonyong, P.; Jobson, M., Flowsheet synthesis and complex distillation column design for separating ternary heterogeneous azeotropic mixtures. *Chem. Eng. Res. Des.* **2011,** *89* (8), 1362-1376.

8. Zhao, L.; Lyu, X.; Wang, W.; Shan, J.; Qiu, T., Comparison of heterogeneous azeotropic distillation and extractive distillation methods for ternary azeotrope ethanol/toluene/water separation. *Comput. Chem. Eng.* **2017,** *100*, 27-37.

9. Chien, I.-L.; Wang, C. J.; Wong, D. S. H., Dynamics and Control of a Heterogeneous Azeotropic Distillation Column: Conventional Control Approach. *Ind. Eng. Chem. Res.* **1999,** *38*, 468-478.

10. Shi, P.; Xu, D.; Ding, J.; Wu, J.; Ma, Y.; Gao, J.; Wang, Y., Separation of azeotrope (2,2,3,3-tetrafluoro-1-propanol + water) via heterogeneous azeotropic distillation by energy-saving dividing-wall column: Process design and control strategies. *Chem. Eng. Res. Des.* **2018,** *135*, 52-66.

11. Hegely, L.; Lang, P., Influence of entrainer recycle for batch heteroazeotropic distillation. *Front. Chem. Sci. Eng.* **2018,** *12* (4), 643-659.

12. Luyben, W. L., Design and Control of a Fully Heat-Integrated Pressure-Swing Azeotropic Distillation System. *Ind. Eng. Chem. Res.* **2008**, 2681-2695.

13. Yang, A.; Lv, L.; Shen, W.; Dong, L.; Li, J.; Xiao, X., Optimal Design and Effective Control of the tert-Amyl Methyl Ether Production Process Using an Integrated Reactive Dividing Wall and Pressure Swing Columns. *Ind. Eng. Chem. Res.* **2017,** *56* (49), 14565-14581.

14. Yang, A.; Shen, W.; Wei, S.; Dong, L.; Li, J.; Gerbaud, V., Design and control of pressure-swing distillation for separating ternary systems with three binary minimum azeotropes.

AIChE J. **2019,** *65* (4), 1281-1293.

15. Modla, G.; Lang, P., Feasibility of new pressure swing batch distillation methods. *Chem. Eng. Sci.* **2008,** *63* (11), 2856-2874.

16. Liang, S.; Cao, Y.; Liu, X.; Li, X.; Zhao, Y.; Wang, Y.; Wang, Y., Insight into pressure-swing distillation from azeotropic phenomenon to dynamic control. *Chem. Eng. Res. Des.* **2017,** *117*, 318-335.

17. An, Y.; Li, W.; Li, Y.; Huang, S.; Ma, J.; Shen, C.; Xu, C., Design/optimization of energy-saving extractive distillation process by combining preconcentration column and extractive distillation column. *Chem. Eng. Sci.* **2015,** *135*, 166-178.

18. You, X.; Gu, J.; Peng, C.; Shen, W.; Liu, H., Improved Design and Optimization for Separating Azeotropes with Heavy Component as Distillate through Energy-Saving Extractive Distillation by Varying Pressure. *Ind. Eng. Chem. Res.* **2017,** *56* (32), 9156-9166.

19. Shen, W.; Dong, L.; Wei, S.; Li, J.; Benyounes, H.; You, X.; Gerbaud, V., Systematic design of an extractive distillation for maximum-boiling azeotropes with heavy entrainers. *AIChE J.* **2015,** *61* (11), 3898-3910.

20. Lo, K.-M.; Chien, I. L., Efficient separation method for tert -butanol dehydration via extractive distillation. *J. Taiwan Inst. Chem. E.* **2017,** *73*, 27-36.

21. Zhao, Y.; Ma, K.; Bai, W.; Du, D.; Zhu, Z.; Wang, Y.; Gao, J., Energy-saving thermally coupled ternary extractive distillation process by combining with mixed entrainer for separating ternary mixture containing bioethanol. *Energy* **2018,** *148*, 296-308.

22. Wang, C.; Guang, C.; Cui, Y.; Wang, C.; Zhang, Z., Compared novel thermally coupled extractive distillation sequences for separating multi-azeotropic mixture of

acetonitrile/benzene/methanol. *Chem. Eng. Res. Des.* **2018,** *136*, 513-528.

23. Graczová, E.; Šulgan, B.; Barabas, S.; Steltenpohl, P., Methyl acetate–methanol mixture separation by extractive distillation: Economic aspects. *Front. Chem. Sci. Eng.* **2018,** *12* (4), 670-682.

24. Gu, J.; You, X.; Tao, C.; Li, J.; Shen, W.; Li, J., Improved design and optimization for separating tetrahydrofuran–water azeotrope through extractive distillation with and without heat integration by varying pressure. *Chem. Eng. Res. Des.* **2018,** *133*, 303-313.

25. Kiss, A. A.; Ignat, R. M., Innovative single step bioethanol dehydration in an extractive dividing-wall column. *Sep. Purifi. Technol.* **2012,** *98*, 290-297.

26. Sun, L.; Wang, Q.; Li, L.; Zhai, J.; Liu, Y., Design and Control of Extractive Dividing Wall Column for Separating Benzene/Cyclohexane Mixtures. *Ind. Eng. Chem. Res.* **2014,** *53* (19), 8120-8131.

27. Timoshenko, A. V.; Anokhina, E. A.; Morgunov, A. V.; Rudakov, D. G., Application of the partially thermally coupled distillation flowsheets for the extractive distillation of ternary azeotropic mixtures. *Chem. Eng. Res. Des.* **2015,** *104*, 139-155.

28. Yang, A.; Wei, R.; Sun, S.; Wei, S.; Shen, W.; Chien, I. L., Energy-Saving Optimal Design and Effective Control of Heat Integration-Extractive Dividing Wall Column for Separating Heterogeneous Mixture Methanol/Toluene/Water with Multiazeotropes. *Ind. Eng. Chem. Res.* **2018,** *57* (23), 8036-8056.

29. Zhao, Y.; Zhao, T.; Jia, H.; Li, X.; Zhu, Z.; Wang, Y., Optimization of the composition of mixed entrainer for economic extractive distillation process in view of the separation of tetrahydrofuran/ethanol/water ternary azeotrope. *J. Chem. Technol. Biot.* **2017,** *92* (9), 2433-2444.

30. Luyben, W. L., Control comparison of conventional and thermally coupled ternary extractive distillation processes. *Chem. Eng. Res. Des.* **2016,** *106*, 253-262.

31. Hsu, K.-Y.; Hsiao, Y.-C.; Chien, I.-L., Design and Control of Dimethyl Carbonate-Methanol Separation via Extractive Distillation in the Dimethyl Carbonate Reactive-Distillation Process. *Ind. Eng. Chem. Res.* **2010,** *49*, 735–749.

32. Momoh, S. O., Assessing the Accuracy of Selectivity as a Basis for Solvent Screening in Extractive Distillation Processes. *Sep. Sci. Technol.* **1991,** *26* (5), 729-742.

33. Tang, Y. T.; Huang, H.-P.; Chien, I.-L., Design of a complete ethyl acetate reactive distillation system. *J. Chem. Eng. Jpn.* **2003,** *36* (11), 1352-1363.

34. Shen, W.; Benyounes, H.; Gerbaud, V., Extension of Thermodynamic Insights on Batch Extractive Distillation to Continuous Operation. 1. Azeotropic Mixtures with a Heavy Entrainer. *Ind. Eng. Chem. Res.* **2013,** *52* (12), 4606-4622.

35. Shen, W.; Gerbaud, V., Extension of Thermodynamic Insights on Batch Extractive Distillation to Continuous Operation. 2. Azeotropic Mixtures with a Light Entrainer. *Ind. Eng. Chem. Res.* **2013,** *52* (12), 4623-4637.

36. Shen, W.; Benyounes, H.; Gerbaud, V., Extractive distillation: recent advances in operation strategies. *Rev. Chem. Eng.* **2015,** *31* (1).

37. Luyben, W. L.; Chien, I.-L., *Design and control of distillation systems for separating azeotropes*. John Wiley & Sons: 2011.

38. Sun, S.; Lü, L.; Yang, A.; Wei, S.; Shen, W., Extractive distillation: Advances in conceptual design, solvent selection, and separation strategies. *Chinese J. Chem. Eng.* **2018**. DOI: 10.1016/j.cjche.2018.08.018

39. Shcherbakova, N.; Rodriguez-Donis, I.; Abildskov, J.; Gerbaud, V., A novel method for detecting and computing univolatility curves in ternary mixtures. *Chem. Eng. Sci.* **2017,** *173*, 21-36.

40. Biegler, L. T.; Cuthrell, J. E., Improved infeasible path optimization for sequential modular simulators—II: the optimization algorithm. *Comput. Chem. Eng.* **1985,** *9* (3), 257-267.

41. Lang, Y.; Biegler, L. T., A unified algorithm for flowsheet optimization. *Comput. Chem. Eng.* **1987,** *11* (2), 143-158.

42. Santaella, M. A.; Jiménez, L. E.; Orjuela, A.; Segovia-Hernández, J. G., Design of thermally coupled reactive distillation schemes for triethyl citrate production using economic and controllability criteria. *Chem. Eng. J.* **2017,** *328*, 368-381.

43. Douglas, J. M., *Conceptual design of chemical processes*. McGraw-Hill New York: 1988; Vol. 1110.

44. Turton, R.; Bailie, R. C.; Whiting, W. B.; Shaeiwitz, J. A., *Analysis, synthesis and design of chemical processes*. Pearson Education: 2008.

45. Zhou, H.; Cai, Y.; You, F., Systems Design, Modeling, and Thermoeconomic Analysis of Azeotropic Distillation Processes for Organic Waste Treatment and Recovery in Nylon Plants. *Ind. Eng. Chem. Res.* **2018,** *57* (30), 9994-10010.

46. Seider, W. D.; Seader, J. D.; Lewin, D. R.; Widagdo, S., *Product and Process Design Principles Synthesis, Analysis and Evaluation*. John Wiley & Sons, Inc.: 2009.

47. Contreras-Zarazúa, G.; Vázquez-Castillo, J. A.; Ramírez-Márquez, C.; Pontis, G. A.; Segovia-Hernández, J. G.; Alcántara-Ávila, J. R., Comparison of intensified reactive distillation configurations for the synthesis of diphenyl carbonate. *Energy* **2017,** *135*, 637-649.

48. Smith, R.; Delaby, O., Targeting flue gas emissions. *Chem. Eng. Res. Des.* **1991,** *69* (6),

492-505.

49. Gadalla, M.; Olujic, Z.; Derijke, A.; Jansens, P., Reducing CO_2 emissions of internally heat-integrated distillation columns for separation of close boiling mixtures. *Energy* **2006,** *31* (13), 2409-2417.

50. Yang, A.; Sun, S.; Eslamimanesh, A.; Wei, S. a.; Shen, W., Energy-saving investigation for diethyl carbonate synthesis through the reactive dividing wall column combining the vapor recompression heat pump or different pressure thermally coupled technique. *Energy* **2019,** *172*, 320-332.

51. Moore, C. F., Selection of controlled and manipulated variables. In *Practical distillation control*, Springer: 1992; pp 140-177.

52. Luyben, W. L., Evaluation of criteria for selecting temperature control trays in distillation columns. *J. Process Contr.* **2006,** *16* (2), 115-134.

53. Hu, Y.; Su, Y.; Jin, S.; Chien, I. L.; Shen, W., Systematic approach for screening organic and ionic liquid solvents in homogeneous extractive distillation exemplified by the tert-butanol dehydration. *Sep. Purifi. Technol.* **2019,** *211*, 723-737.

54. Tyreus, B. D.; Luyben, W. L., Tuning PI controllers for integrator/dead time processes. *Ind. Eng. Chem. Res.* **1992,** *31* (11), 2625-2628.

55. Zhang, X.; Zhao, Y.; Wang, H.; Qin, B.; Zhu, Z.; Zhang, N.; Wang, Y., Control of a Ternary Extractive Distillation Process with Recycle Splitting Using a Mixed Entrainer. *Ind. Eng. Chem. Res.* **2017,** *57* (1), 339-351.

56. Gil, I. D.; Gómez, J. M.; Rodríguez, G., Control of an extractive distillation process to dehydrate ethanol using glycerol as entrainer. *Comput. Chem. Eng.* **2012,** *39*, 129-142.

57. Wang, C.; Wang, C.; Cui, Y.; Guang, C.; Zhang, Z., Economics and Controllability of Conventional and Intensified Extractive Distillation Configurations for Acetonitrile/Methanol/Benzene Mixtures. *Ind. Eng. Chem. Res.* **2018,** *57* (31), 10551-10563.

58. Feng, Z.; Shen, W.; Rangaiah, G. P.; Dong, L., Proportional-Integral Control and Model Predictive Control of Extractive Dividing-Wall Column Based on Temperature Differences. *Ind. Eng. Chem. Res.* **2018,** *57* (31), 10572-10590.

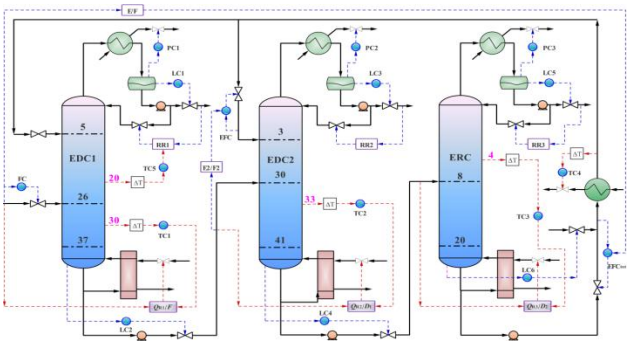

Only for Table of Content (TOC)